PCCP

Physical Chemistry Chemical Physics

www.rsc.org/pccp

Volume 15 | Number 35 | 21 September 2013 | Pages 14513–14824

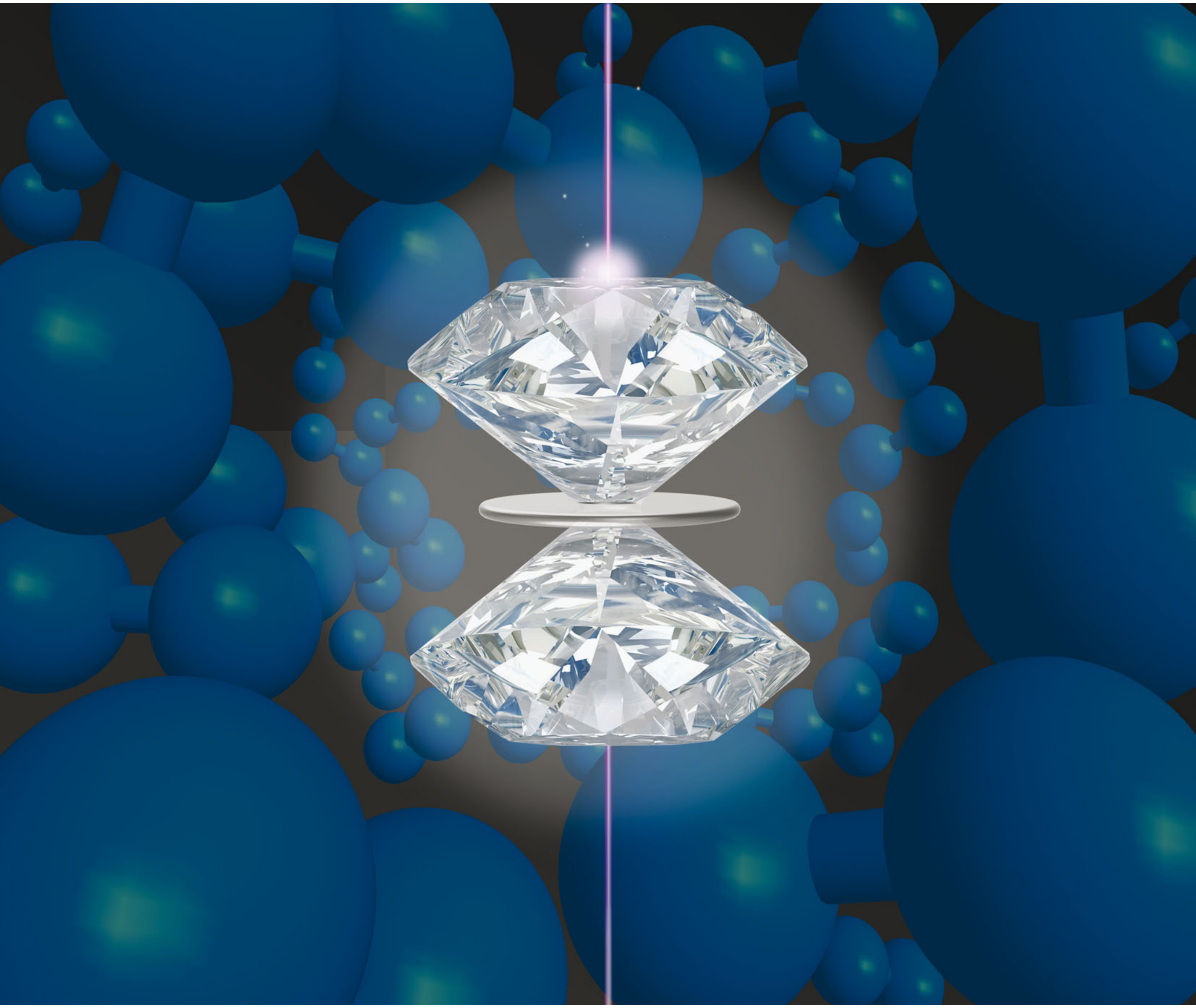

ISSN 1463-9076

PERSPECTIVE
Song
New perspectives on potential hydrogen storage materials using high pressure

1463-9076(2013)15:35;1-K

PCCP

RSC Publishing

PERSPECTIVE

View Article Online
View Journal | View Issue

Cite this: *Phys. Chem. Chem. Phys.*, 2013, **15**, 14524

New perspectives on potential hydrogen storage materials using high pressure

Yang Song*

Received 22nd May 2013,
Accepted 23rd May 2013

DOI: 10.1039/c3cp52154k

www.rsc.org/pccp

In addressing the global demand for clean and renewable energy, hydrogen stands out as the most suitable candidate for many fuel applications that require practical and efficient storage of hydrogen. Supplementary to the traditional hydrogen storage methods and materials, the high-pressure technique has emerged as a novel and unique approach to developing new potential hydrogen storage materials. Static compression of materials may result in significant changes in the structures, properties and performance that are important for hydrogen storage applications, and often lead to the formation of unprecedented phases or complexes that have profound implications for hydrogen storage. In this perspective article, 22 types of representative potential hydrogen storage materials that belong to four major classes—simple hydride, complex hydride, chemical hydride and hydrogen containing materials—were reviewed. In particular, their structures, stabilities, and pressure-induced transformations, which were reported in recent experimental works together with supporting theoretical studies, were provided. The important contextual aspects pertinent to hydrogen storage associated with novel structures and transitions were discussed. Finally, the summary of the recent advances reviewed and the insight into the future research in this direction were given.

Department of Chemistry, University of Western Ontario, London, ON N6A 5B7, Canada. E-mail: yang.song@uwo.ca; Tel: +1-519-661-2111 Ext 86310

Yang Song

Dr Yang Song received his BSc in Chemistry from Peking University, China, in 1997 and PhD in Physical Chemistry from Iowa State University in 2001. After a postdoctoral and research associate position at Harvard and Carnegie Institution of Washington, respectively, he joined the faculty at the University of Western Ontario (Western), Canada, as an Assistant Professor in 2005. He is currently an Associate Professor in the Department of Chemistry at Western. In 2007, he received an Early Researcher Award (ERA) from Ontario Ministry of Research and Innovation. More recently, he was named the 2010–2011 "Petro-Canada Young Innovator" at Western. His research focuses on chemistry and materials under extreme conditions using spectroscopy and synchrotron radiation.

1. Introduction

Hydrogen, which has the highest energy density by weight with the combustion product of H_2O being the only product, has been identified as the next generation clean and renewable energy source for a variety of applications, especially as an on-board fuel for vehicles (*e.g.*, hydrogen powered fuel cell vehicles).[1] However, the commercialization of hydrogen fueled vehicles is still limited by many practical and technological factors, such as those related to the production and distribution as well as the storage of this fuel source within a reasonable pressure and temperature range. The hydrogen storage issue has especially presented a major challenge and, thus, it has received intensive scientific and technological attention over the past decade.[2] Among these investigations, many standards for effective storage have been established, such as high gravimetric and volumetric capacities, reversibility, mild pressure–temperature conditions, reasonable kinetics, and other application-related factors such as cost and environmental impact. To guide the scientific and technological effort to develop effective hydrogen storage systems, the US Department of Energy (DOE) has announced (and updated) the targets for onboard hydrogen storage systems for light-duty vehicles, such as a 5.5 wt% gravimetric capacity or a 40 g H_2 per L volumetric capacity by the year 2017 and an aggressive ultimate respective target of 7.5 wt% H_2 or 70 g H_2 per L.[3]

Hydrogen as a gas has only a density of 0.09 g L^{-1} under standard temperature and pressure conditions. When liquefied, hydrogen exhibits a modest density of 70 g L^{-1}. But the extremely low condensation temperature of 20 K makes the energy consumption for liquidation substantial. Alternatively, hydrogen can be stored as a compressed gas under ~35 MPa at room temperature with 15 g H_2 per L. However, such an approach may not be cost effective because the resulting product will have a low energy density, and there are some safety issues. Therefore, considerable effort has been directed toward materials-based hydrogen storage methods. There are typically two types of mechanisms for hydrogen storage: physisorption and chemisorption. In the first category, hydrogen binds to the storage materials that have a large surface area *via* van der Waals interactions. Examples in this category include carbon-based nanostructures and metal–organic frameworks (MOFs).[4] On the other hand, the atomic binding of hydrogen to the storage materials through covalent, ionic or metallic bonds constitutes the chemisorptive hydrogen storage. This category typically involves hydrogen-rich materials, often referred to as hydrides. Depending on the identity of the non-hydrogen moiety of the materials, hydrides can be further classified as (1) simple hydrides, (2) complex hydrides, or (3) chemical hydrides. Excellent recent review articles are available in which the structures, properties as well as the hydrogen storage performance of these materials are discussed.[5–11]

More recently, an interdisciplinary approach with implications for the development of new and improved hydrogen storage materials has emerged, that is, using extremely high pressures (*e.g.*, in the gigapascal range). The application of high pressure to matter significantly alters the interatomic distances, and thus, the energy landscape by influencing the nature of the intermolecular interactions, the chemical bonding, the molecular configurations, the crystal structures and the stability of materials. New classes of materials having unusual stoichiometries and crystal structures, which have a wide range of novel optical, mechanical, electronic and magnetic properties, have been produced at high pressures.[12,13] Being the simplest and most abundant element in the universe, for example, hydrogen itself has been intensively investigated at extremely high pressures.[14,15] It has long been predicted to be a metallic monoatomic solid above certain pressures (*e.g.*, megabars) and even to exhibit exotic quantum states such as a metallic superfluid and a high-temperature superconductor.[16–19] As a result, the metallization of hydrogen has been the sought-after target that has received a tremendous amount of experimental and theoretical effort in the past several decades.[20–43] While both progressive evidence and contradictive arguments were reported with respect to the target,[21,24,27,29,31,39,42,43] the conclusions remain controversial,[44] leaving the high-pressure investigation of hydrogen to remain as a long-lasting topic.

More significantly, the high-pressure development of functional materials with potential industrial applications, such as high-energy-density materials, superhard materials and hydrogen storage materials, has become a vibrant area of high-pressure research.[45] Analogous to the well-known ''flammable ice'' where methane forms a stable hydrate complex with ice under extreme pressure and temperature conditions, for example, hydrogen can be trapped in water cages to form clathrate hydrate at high pressures as well (more details are provided later),[46] shedding new light on hydrogen storage applications. Over the years, there has been an increasing number of examples of pressure-induced formation of new classes of hydrogen containing complexes.

In this perspective article, we discuss this unique aspect of the high-pressure investigation of potential hydrogen storage materials, mainly focusing on hydrogen-rich materials, *i.e.*, hydrides. Not only has pressure demonstrated great promise for producing new structures and materials, but also many known hydrogen-rich materials have exhibited new transformations as well as totally different thermodynamic and kinetic behaviors under higher pressures than those present under ambient conditions. The large volume of recent high-pressure experimental and theoretical studies has revealed new knowledge that could be the foundation for further development of hydrogen storage materials starting from these precursors. In the following examination, we review only those hydrides that have been studied at high pressures *experimentally* (and discuss the available computational studies but we do not include materials that have been only studied hypothetically) in six categories:[47] (1) simple hydrides; (2) alanates; (3) borohydrides; (4) amides; (5) chemical hydrides; and (6) hydrogen-containing complexes. The included materials and systems are summarized in Table 1.

2. Simple hydrides

The term, simple hydrides, mostly refers to binary metal hydrogen compounds with a formula of MH_x formed by the direct reaction between molecular hydrogen and the metal (M). The chemically stored hydrogen can be released as molecular hydrogen in the reverse reaction at certain temperatures. Because of their light weight, alkali and alkaline earth metals are typically used for hydrogen storage applications. In these compounds, due to the larger electronegativity of hydrogen, the metal–hydrogen bond is considered to be ionic in nature. The interaction in other types of simple metal hydrides, such as in transition metal hydrides, however, is considered to be metallic or interstitial. In these cases, the hydrides are interstitial alloys that are formed between the metal and the hydrogen atom since the metal remains in its original crystal lattice positions while the hydrogen is inserted into its interstitial sites. Here we review only the former case, and include only those hydrides that have been studied at high pressures, *e.g.*, LiH, NaH, MgH_2, AlH_3, and CaH_2.[48]

2.1 LiH

Lithium hydride (LiH) is the simplest and lightest hydride of all kinds containing a desirable hydrogen content of 12.6%. Despite the high hydrogen content, the irreversible kinetics and high hydrogen discharge temperature (*i.e.*, ~1000 K) limit

Table 1 Summary of materials and systems for hydrogen storage investigated at high pressures

Materials	Maximum hydrogen content[a]	Structural information	Pressure range[b] (GPa)	Temperature range[b] (K)	Method[c]	References
Simple hydride						
LiH	12.6%	$Fm\bar{3}m$	250	Room	XRD, ND, RS, AB	49–51
NaH	4.2%	$Fm\bar{3}m$ (B1); $Pm\bar{3}m$ (B2)	54	Room	XRD, AB	60
MgH_2	7.6%	$P4_2/mnm$ (α); $Pa\bar{3}$ (β); $Pbcn$ (γ); $Pbca$ (δ′)	16	1070	XRD, ND, AB	64, 65 and 67
CaH_2	4.8%	$Pnma$; $P6_3/mmc$	42	Room	XRD, RS, AB	72 and 73
AlH_3	10.0%	$R\bar{3}c$ (α); $Cmcm$ (α′); $Fd\bar{3}m$ (β); $Pnnm$ (γ); $P2$ (α-II); $Pm\bar{3}n$ (α-III)	164	4	XRD, ND, RS, AB	79–83, 87, 88, 90 and 92
Complex hydride						
$LiAlH_4$	10.5%	$P2_1/c$ (α); $I2/b$ (β)	7	773	XRD, ND, RS, AB	94, 98–101 and 104
$NaAlH_4$	7.4%	$I4_1/a$ (α); $P2_1/c$ (β)	27	Room	XRD, RS, AB	106–108 and 110
$LiBH_4$	18.4%	$Pnma$ (α or II); $P6_3mc$ (I); $Ama2$ (β or III); $Fm\bar{3}m$ (V)	10	500	XRD, ND, RS, AB	116–120
$NaBH_4$	10.6%	$Fm\bar{3}m$ (α); $P\bar{4}2_1c$ (β); $Pnma$ (γ)	30	80–673	XRD, IXS, INS, RS, AB	129–136 and 141
KBH_4	7.4%	$Fm\bar{3}m$ (α); $P\bar{4}2_1c$ (β); $Pnma$ (γ)	20	Room	XRD, RS, AB	144
$Ca(BH_4)_2$	11.5%	$Fddd$ or $F2dd$ (α); $P\bar{4}$ or $P4_2/m$ (β); $Pbca$ (γ); $I\bar{4}2d$ (α′)	10	873	XRD, ND, INS, RS, IR, AB	153–158, 160–163 and 165
$LiNH_2$	8.8%	$I\bar{4}$ (α); $P2_1$ (β)	28	Room	XRD, RS, AB	167, 171 and 172
$NaNH_2$	5.2%	$Fddd$	16	Room	RS, AB	176
Chemical hydride						
B_2H_6	22%	$P2_1/n$(β)	50	Room	RS, IR, AB	180 and 181
NH_3BH_3	19%	$I4mm$; $Pmn2_1$; $Cmc2_1$; $P2_1$	65	15–350	XRD, ND, INS, RS, IR, AB	196, 198, 200, 201, 204–210 and 212–216
H_2 containing complex						
CH_4–H_2	33% (50%)	$CH_4(H_2)_2$; $(CH_4)_2H_2$; $CH_4(H_2)_4$; CH_4H_2	60	10	XRD, RS, IR, AB	221–223
H_2O–H_2	10% (20%)	C_1; C_2; sII	80	10–450	XRD, ND, RS, AB	46, 225, 229–237, 239, 241, 244–246, 249 and 251
SiH_4–H_2 & GeH_4–H_2	11% (22%)	$SiH_4(H_2)_2$ – $F\bar{4}3m$	10 & 27	Room	XRD, RS, IR, AB	256, 257 and 267
NH_3BH_3–H_2	12% (29%)	NH_3BH_3 $(H_2)_x$, $x \cong 1.3$–2	60	413	RS	270–272
Ar–H_2 & Xe–H_2	9% & 9.7%	$Ar(H_2)_2$ – $P6_3/mmc$; $Xe(H_2)_7$ – $R3$	200 & 255	Room	XRD, RS, IR, AB	274–280 and 284–286

[a] For the H_2 containing complex, the data in the parentheses refer to the overall hydrogen content instead of the stored hydrogen only. [b] The data for the pressure and temperature range are only from experimental work. For pressure, the range refers to going from the ambient to the given value; for temperature, unless labeled "Room", *i.e.*, at 298 K, the values refer to either the maximum or the minimum or to a range of temperatures under which the materials were investigated under simultaneous high pressure conditions. [c] XRD: X-ray diffraction; IXS: inelastic X-ray scattering; ND: neutron diffraction; INS: inelastic neutron scattering; RS: Raman spectroscopy; IR: infrared spectroscopy; AB: *ab initio* calculations.

its hydrogen storage applications. Under ambient conditions, it crystallizes into a cubic structure with the space group of $Fm\bar{3}m$ (also known as a B1 rocksalt structure, Fig. 1a) and has a cell parameter of a = 4.08 Å and a density of 0.78 g cm^{-3}.[49] Over the past few decades, LiH has undergone numerous experimental investigations such as those by X-ray diffraction, neutron diffraction, and Raman spectroscopy, as well as theoretical studies about its high-pressure structures and properties.[50–57] In addition, its isotopic substituted compound LiD has been comparatively investigated at high pressures. Using single crystal synchrotron X-ray diffraction, for example, Loubeyre *et al.* examined the high pressure behavior of LiH up to 36 GPa (and 94 GPa for LiD).[51] In their experiment, no phase transitions were observed over the entire pressure range and the LiH retained the B1 structure. Driven by the pursuit of other interesting properties of LiH at high pressures—such as lower symmetry and electrode structures, low-temperature melting, as well as metallization—numerous theoretical studies on LiH were performed.[53–58] The *ab initio* calculations suggest that the B1 structure will remain stable up to at least 226 GPa before a possible transition from B1 to B2 (with space group $Pm\bar{3}m$).[58] More recently, Lazicki *et al.* performed static compression of LiH up to 250 GPa characterized by X-ray diffraction and Raman spectroscopy.[59] Their results further confirmed that the long predicted B1-to-B2 transition should occur far beyond the currently achieved pressure threshold. All the experimental and *ab initio* studies suggested a bulk modulus of LiH in the range of 30–35 GPa, indicating that LiH is highly compressible. The extremely high structural stability and compressibility of LiH suggest that LiH by itself may have limited application for hydrogen storage, but it may play a role when combined with other metal hydrides in the form of complex hydrides (see following discussion).

2.2 NaH

Sodium hydride (NaH) has a relatively lower weight capacity of 4.2 wt% H_2. However, it also has a much lower decomposition temperature than LiH, *i.e.*, 698 K, and has relatively good reversible kinetics. It crystallizes into a cubic crystal system, with the same structure as LiH, *i.e.*, $Fm\bar{3}m$, under ambient conditions.

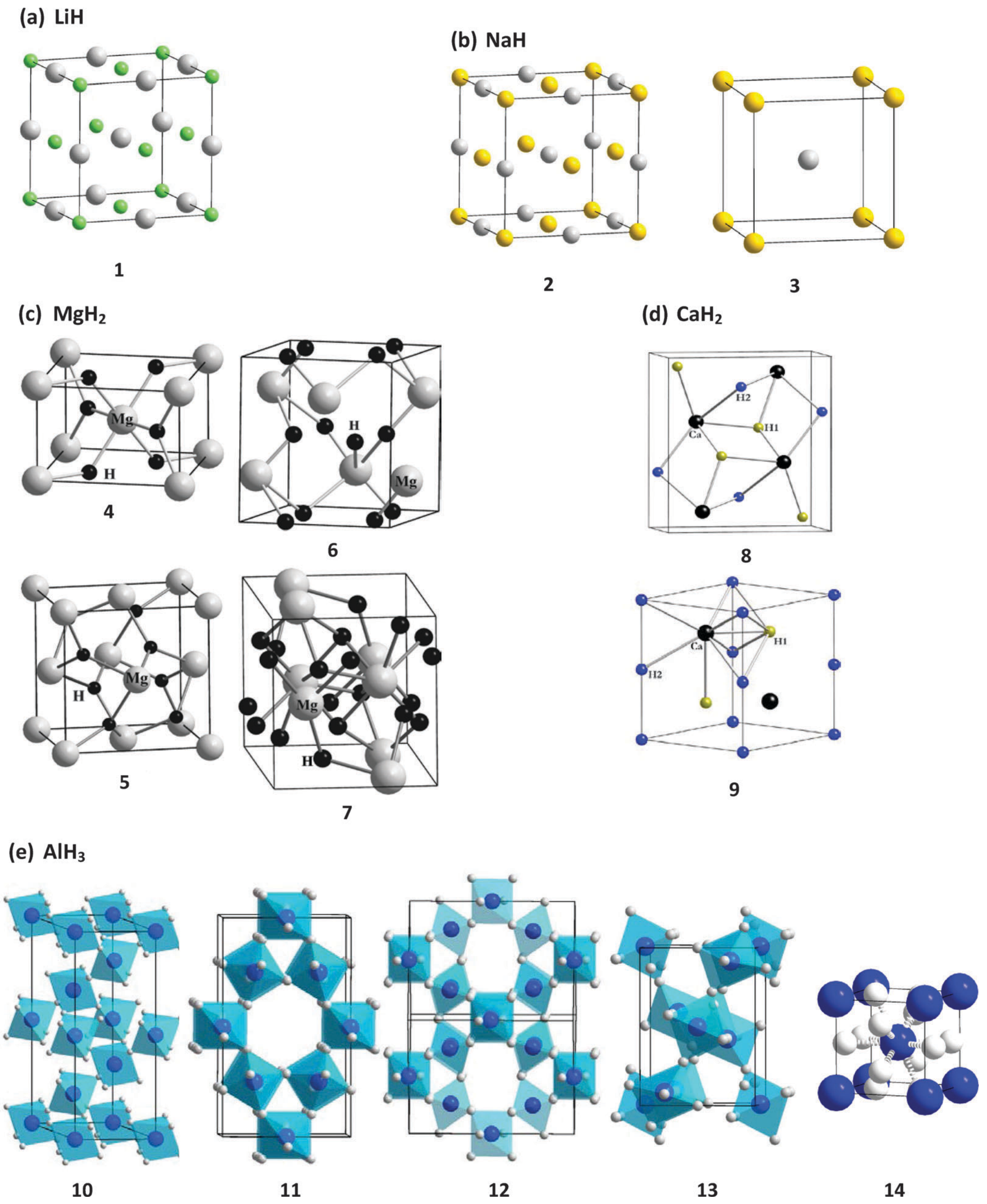

Fig. 1 Crystal structures of simple hydrides. The space groups for different phases and presentation legends are: (a) LiH (**1**: $Fm\bar{3}m$), H: white, Li: green; (b) NaH (**2**:, $Fm\bar{3}m$ (B1 phase); **3**: $Pm\bar{3}m$ (B2 phase)), H: grey, Na: yellow; (c) MgH_2 (**4**: $P4_2/mnm$ (α phase); **5**: $Pa\bar{3}$ (β phase); **6**: *Pbcn* (γ phase); **7**: *Pbca* (δ′ phase)), reproduced with permission.[67] Copyright 2006 American Physical Society; (d) CaH_2 (**8**: *Pnma*; **9**: $P6_3/mmc$), reproduced with permission.[74] Copyright 2008 IOP Publishing; (e) AlH_3 (**10**: $R\bar{3}c$ (α phase); **11**: *Cmcm* (α′ phase); **12**: $Fd\bar{3}m$ (β phase); **13**: *Pnnm* (γ); **14**: $Pm\bar{3}n$ (high-P phase III)), H: grey, Al: blue.

Using synchrotron X-ray diffraction, Duclos *et al.* studied NaH at pressures of up to 54 GPa and observed the expected B1-to-B2 phase transition at a pressure of ∼30 GPa (the B1 and B2 structures of NaH are shown in Fig. 1b).[60] The bulk modulus was found to be lower than LiH as well, *i.e.*, ∼20 GPa. In this study, the trends of phase transition pressure and compressibility in alkali metal hydrides were further established, *i.e.*, lower transition pressures and higher compressibilities for heavier alkaline metals. However, due to its very low hydrogen content, NaH has not received as much attention as LiH until recently. Using *ab initio* calculations, Baettig and Zurek showed that it is possible to produce and pressure-stabilize a sodium hydride compound with a much higher hydrogen content, *e.g.*, sodium polyhydride (NaH_n, $n > 1$) at pressures of up to 25 GPa.[61] Their findings shed new light on the sodium hydride based hydrogen storage materials.

2.3 MgH_2

With 7.6 wt% H_2, magnesium hydride (MgH_2) can be obtained from the relatively cheap magnesium metal and, thus, has been extensively investigated as a hydrogen storage agent.[62,63]

Although the decomposition temperature of 603 K was considered to be relatively low, the poor reversibility and kinetics were found to be major issues for direct application in hydrogen storage.[63] Under ambient conditions, it crystallized into a rutile structure (space group $P4_2/mnm$, Fig. 1c, **4**), known as α-MgH_2.[64] At high pressures, MgH_2 exhibits rich polymorphs. In 1999, Bortz *et al.* reported the formation of γ-MgH_2 by heating α-MgH_2 in a multianvil press at a pressure of 2 GPa and a temperature of 1070 K followed by rapid quenching.[65] Using X-ray and neutron powder diffraction, the γ-MgH_2 was determined to have an α-PbO_2 type structure (space group *Pbcn*, Fig. 1c, **6**). In 2002, Vajeeston *et al.* employed density functional theory to investigate the pressure-induced transitions of MgH_2, in which the α-to-γ transition was reproduced and similar stabilities of the two phases were reported.[66] Furthermore, a γ- to β-MgH_2 transition was predicted at 3.8 GPa, as well as other possible structural transitions at higher pressures. Subsequent high pressure experiments with pressures of up to 16 GPa by the same group confirmed the previous predictions and solved the structures of the new phases, including β and δ′ with the respective structures of the modified CaF_2 ($Pa\bar{3}$) and $AuSn_2$ types (*Pbca*) (see Fig. 1c, **5** and **7**).[67] Later *ab initio* calculations by Cui *et al.* also suggested other phases such as ε and δ, which, however, have not been experimentally confirmed.[68] More recently, Moser *et al.* updated the pressure–temperature phase diagram of MgH_2 based on computational thermodynamics using density functional theory.[69] Understanding the structural stability and bonding nature of MgH_2 is considered essential to improving its hydrogen storage properties. All of the experimental and first principles calculations suggest that all phases of MgH_2 have a strong ionic character as alkali metal hydrides. Thus, making its ionic bonding weaker, for example, by pressure modification and/or with other dopants, is a possible way to improve the dehydrogenation performance of MgH_2.

2.4 CaH_2

Calcium hydride (CaH_2) contains only 4.8 wt% H_2 and has a relatively high decomposition temperature of 873 K. Therefore, it is rarely used as the hydrogen storage agent by itself despite its relatively good reversible kinetics.[70] However, CaH_2 has been reported to be a good destabilizer for other agents, *e.g.*, $NaBH_4$ in hydrogen storage applications.[71] Under ambient conditions, CaH_2 crystallizes into an orthorhombic structure (space group *Pnma*, Fig. 1d, **8**). And at high pressure, only two experimental works are available. Using Raman spectroscopy aided by *ab initio* calculations, Li *et al.* reported a reversible phase transition at around 15 GPa where the high-pressure phase was found to be stable up to 42 GPa.[72] Tse *et al.* confirmed the phase transition using Raman spectroscopy, synchrotron X-ray diffraction and first principle calculations, and identified the high pressure structure as being $P6_3/mmc$ (Fig. 1d, **9**).[73] Some other theoretical work has also been reported to interpret the crystal structures, electronic and dynamic properties, compressibilities, and the transition mechanism as well as to predict other possible high pressure structures.[74]

2.5 AlH_3

Aluminum hydride, or alane (AlH_3), has a high gravimetric hydrogen capacity of 10.0% and a volumetric content of 148 g L^{-1}, respectively. In addition, it has a low dehydrogenation temperature (*i.e.*, 423 K) and other desirable properties for onboard hydrogen storage, such as the low cost of the aluminum metal and little environmental impact.[75,76] However, the production of AlH_3, or the hydrogenation process, typically requires the application of high pressure and other extreme conditions.[77] These requirements are a limiting factor in using alane as a practical hydrogen storage material. Therefore, some alternative methods to produce alane have been pursued with success.[78]

Alane has rich crystal structures with several known polymorphs depending on the synthetic route. Using X-ray and neutron diffraction as well as spectroscopic techniques, the crystal and electronic structures for four phases (α, α′, β and γ) have been characterized for AlH_3 (or AlD_3).[79–87] As the most stable phase, α-AlH_3 has a trigonal structure (space group $R\bar{3}c$) with corner sharing of the [AlH_6] octahedra (Fig. 1e, **10**). The α′ phase takes on the α-AlF_3 orthorhombic structure with space group *Cmcm* – also with corner-sharing [AlH_6] octahedra but in an open structure with hexagonal holes (Fig. 1e, **11**). The β-AlH_3 has a pyrochlore-type crystal structure (space group $Fd\bar{3}m$) with the [AlH_6] octahedral arrangement with an open framework in several directions (Fig. 1e, **12**). The γ-AlH_3 adopts an orthorhombic unit cell with a space group *Pnnm* where two-thirds of the [AlH_6] octahedra are both corner- and edge-sharing (Fig. 1e, **13**). Among these four polymorphs, the α phase has the highest density and the β-AlH_3 has the lowest.

At high pressures, α-AlH_3 has been studied by Raman spectroscopy and synchrotron X-ray diffraction.[79,88–92] In the early studies at relatively lower pressures (*i.e.*, up to 7 GPa), no phase transitions were observed indicating the high stability.[79,88] When compressed to extremely high pressures (*e.g.*, above 100 GPa), two phase transitions were observed at 60 and 100 GPa, respectively, resulting in the formation of two new high pressure phases: monoclinic *P*2 (phase II) and cubic $Pm\bar{3}n$ (phase III).[89] The $Pm\bar{3}n$ phase is a metallic phase with a remarkably simple cubic structure with Al atoms residing at (0, 0, 0) and $(\frac{1}{2}, \frac{1}{2}, \frac{1}{2})$ positions coordinated with 12 H atoms, whose shortest first-neighbor H–H distances are just next to that in the H_2 molecule (Fig. 1e, **14**). Using Raman spectroscopy and synchrotron X-ray diffraction, Drozd *et al.* studied β-AlH_3 at high pressures.[92] The β-AlH_3 was found to be stable up to 6 GPa before a subsequent transformation to an α phase at higher pressures occurred. Vajeeston *et al.* employed first principles calculations on the high pressure behavior of β-AlH_3 and predicted a sequence of phase transitions of β → α′ → α → hp1 ($P6_3/m$) → hp2 ($Pm\bar{3}n$).[91] While the high pressure phase hp2 is consistent with the experimental result obtained by Goncharenko *et al.*,[89] the other high pressure phase hp1 has not been experimentally confirmed yet. In both Tkacz's and Drozd's Raman studies on γ-AlH_3, it was also found that γ-AlH_3 transforms irreversibly into the more stable α phase at above 12 GPa.[90,92] In addition, Drozd *et al.* discovered that the γ-AlH_3 is subject to X-ray radiation-induced decomposition into its constituent elements at 15 GPa. All of these observations suggest that the α phase is much more stable than the other phases; while the less stable β and γ phases with open framework structures may play a more interesting role in hydrogen storage applications at high pressures.

3. Alanates

Alanates are a class of complex metal hydrides with a general formula of [$M(AlH_4)_x$], where M is typically alkali or alkaline earth metals, such as Li, Na, K, Mg, and Ca. Due to their high gravimetric hydrogen content, alanates have been considered to be promising hydrogen storage materials that release hydrogen *via* the following reactions:[7,93–95]

$$3MAlH_4 \rightarrow M_3AlH_6 + 2Al + 3H_2 \quad (1)$$

$$M_3AlH_6 \rightarrow 3MH + Al + 3/2H_2 \quad (2)$$

In alanates, the alkali or alkaline earth metals carry a positive charge, and, thus, interact with the [AlH_4] group ionically. The AlH_4^- anion is formed by the covalent Al–H bond, which plays an important role in the hydrogen discharge and storage processes.[96] Under pressure, the charge distribution as well as the metal–hydrogen bond can be significantly influenced and, thus, the stability, and the dynamics as well as the kinetics of alanates may be completely different. Although many alanates are available either commercially or through a synthetic route, only $LiAlH_4$ and $NaAlH_4$ have been investigated under high pressure.[97] Thus, in the following section we only review these two alanates.

3.1 $LiAlH_4$

Lithium alanate ($LiAlH_4$) has a high gravimetric hydrogen capacity of 10.5 wt% H_2 and, thus, has been extensively studied for hydrogen storage. However, two major issues are the slow kinetics and the poor hydrogenation–dehydrogenation reversibility.[93] As a result, extensive effort has been made to improve these aspects, such as to use a Ti-based dopant or catalyst.[7] Under ambient conditions, $LiAlH_4$ exists in the α-phase with a monoclinic structure (space group $P2_1/c$, Fig. 2a, **1**).[98] Using Raman spectroscopy, Talyzin and Sundqvist observed a slow and reversible phase transition from α to β phase between 2.2 and 3.5 GPa.[99] Chellappa *et al.* reproduced the Raman results and further established that the β-$LiAlH_4$ has a distorted [AlH_4^-] tetrahedron.[100] More significantly, the softening of the Al–H stretching mode suggests the weakening of the Al–H bond that may have important implications for hydrogen storage. Later, using *in situ* time-of-flight neutron diffraction at high pressures, Pitt *et al.*[101] resolved the crystal structure of $LiAlH_4$ (in the form of $LiAlD_4$) as a monoclinic space group $I2/b$ (Fig. 2a, **2**). Using *ab initio* calculations, Vajeeston *et al.*[102] predicted other pressure induced phase transitions such as from β- to γ-$LiAlH_4$ at 33.8 GPa, which have not been experimentally observed yet.[103] Very recently, Fallas *et al.* mapped out the pressure–temperature phase diagram by combining their Raman measurements together with data taken from the previous literature (Fig. 2b).[104]

3.2 $NaAlH_4$

With 7.4 wt% H_2, sodium alanate ($NaAlH_4$) has a similar hydrogen storage performance and mechanism to that of $LiAlH_4$, but it has a higher decomposition temperature (*i.e.*, ∼523 K) than $LiAlH_4$. Nonetheless, enhanced absorption–desorption kinetics and reversible hydrogenation–dehydrogenation can be achieved by using a transition metal (*e.g.*, Ti) based catalyst, giving promising practical hydrogen storage applications.[105] Under ambient conditions, $NaAlH_4$ crystallizes into a tetragonal space group $I4_1/a$ (known as the α-phase) with a distorted [AlH_4] tetrahedron (Fig. 2a, **3**). Using Raman spectroscopy, Talyzin and Sundqvist observed a reversible pressure-induced phase transition from α to β at around 14–16 GPa.[106] Subsequently, Kumar *et al.*[107] reported *in situ* Raman spectroscopy and synchrotron X-ray diffraction studies of $NaAlH_4$ at pressures of up to 27 GPa, where β-$NaAlH_4$ was determined to have a $P2_1/c$ monoclinic structure (Fig. 2a, **4**) that is 12% denser than the α phase. However, it was found that the ball-mill synthesized $NaAlH_4$ undergoes a reversible pressure-induced amorphization at 6.5–13.5 GPa as characterized by synchrotron X-ray diffraction.[108] Several theoretical studies[109–112] on other possible high pressure structures of $NaAlH_4$ were also reported with important structural implications for dehydrogenation mechanisms, such as the prediction of a γ-phase and a new high pressure phase of *Ima*2 above 20 GPa,[111] but no experimental evidence is available yet.

4. Borohydrides

Alkali and alkaline earth borohydrides [$M(BH_4)_n$], where M = Li, Na, K and $n = 1$; or M = Mg, Ca and $n = 2$, are another class of complex metal hydrides that have extensive hydrogen storage applications due to their light weight and high hydrogen content.[113] However, this class of complex metal hydrides generally has a very high decomposition temperature due to the strong covalent bonds in BH_4^- and the ionic bonds between the metal and BH_4^-. Therefore, much effort has been made to "destabilize" the agent, for example, by introducing a catalyst or by using compositional modification *via* reacting with another metal hydride.[7] Many excellent review articles about the progress on borohydride based hydrogen storage systems are available.[8–10] Here, we only review those that have been investigated in high pressure experiments, *i.e.*, $LiBH_4$, $NaBH_4$, KBH_4, and $Ca(BH_4)_2$.[114]

4.1 $LiBH_4$

Lithium borohydride ($LiBH_4$) has a very high gravimetric hydrogen capacity of 18.4 wt%. The dehydrogenation of $LiBH_4$ yields a 13.9% H_2 *via* reaction (3), while an important intermediate species has been identified that may produce a different dehydrogentation yield *via* reaction (4).[115]

$$LiBH_4 \rightarrow LiH + B + 3/2H_2 \quad (3)$$

$$LiBH_4 \leftrightarrow 1/12Li_2B_{12}H_{12} + 5/6LiH + 13/12H_2 \leftrightarrow LiH + B + 3/2H_2 \quad (4)$$

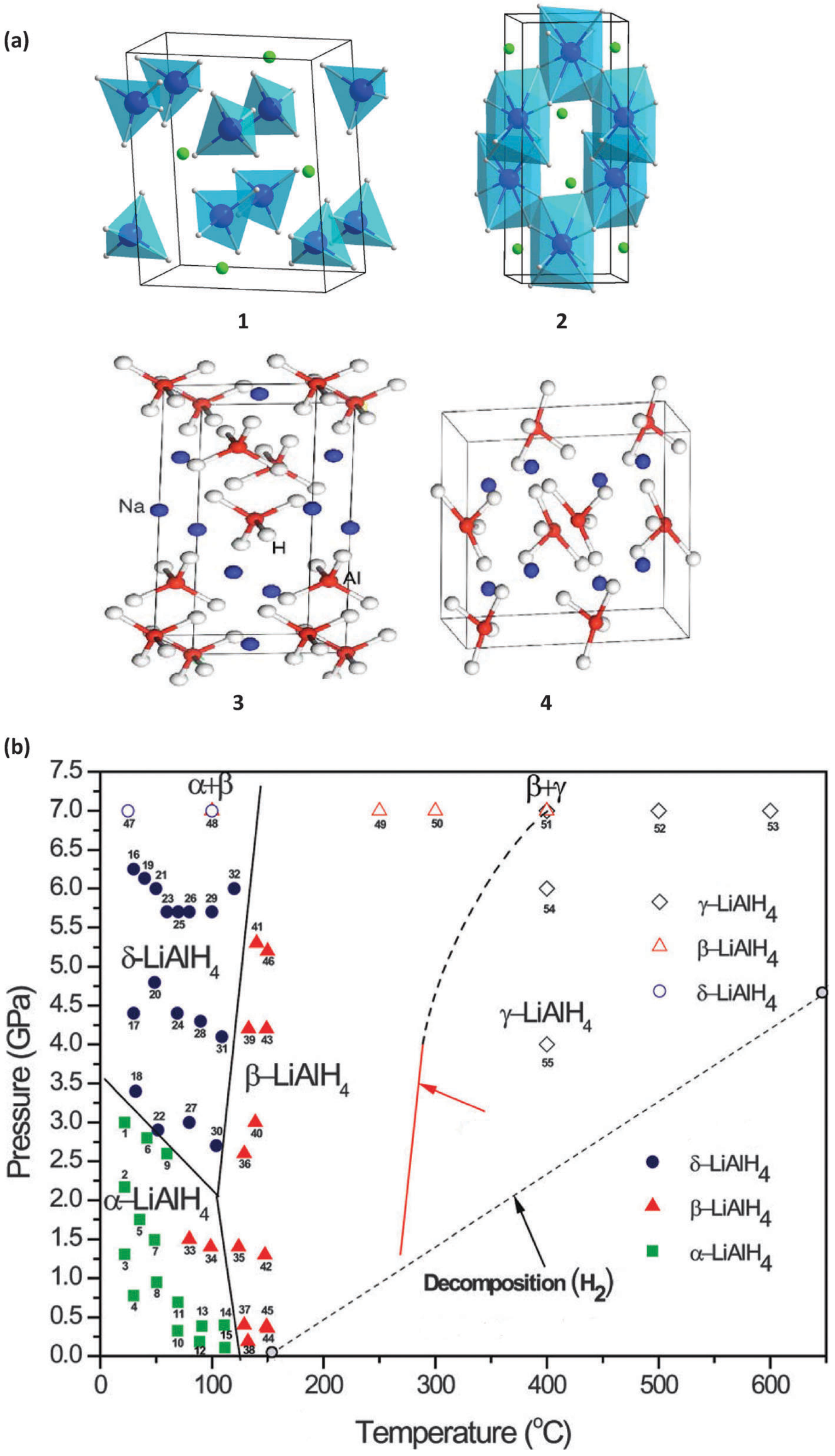

Fig. 2 (a) Crystal structures of $LiAlH_4$ (**1**: space group $P2_1/c$ (α phase) and **2**: space group $I2/b$ (β phase), atom colors: H: white; Al: blue; Li: green) and $NaAlH_4$ (**3**: space group $I4_1/a$ (α phase) and **4**: space group $P2_1/c$ (β phase)). (b) Pressure–temperature phase diagram of $LiAlH_4$. Reproduced with permission.[104] Copyright 2010 American Chemical Society.

Under ambient conditions, $LiBH_4$ crystallizes into an orthorhombic structure with a space group of *Pnma* (known as the α phase or phase II, Fig. 3a, **1**) with the $[BH_4^-]$ tetrahedron strongly distorted.[116] Upon heating to 408 K, a temperature-induced

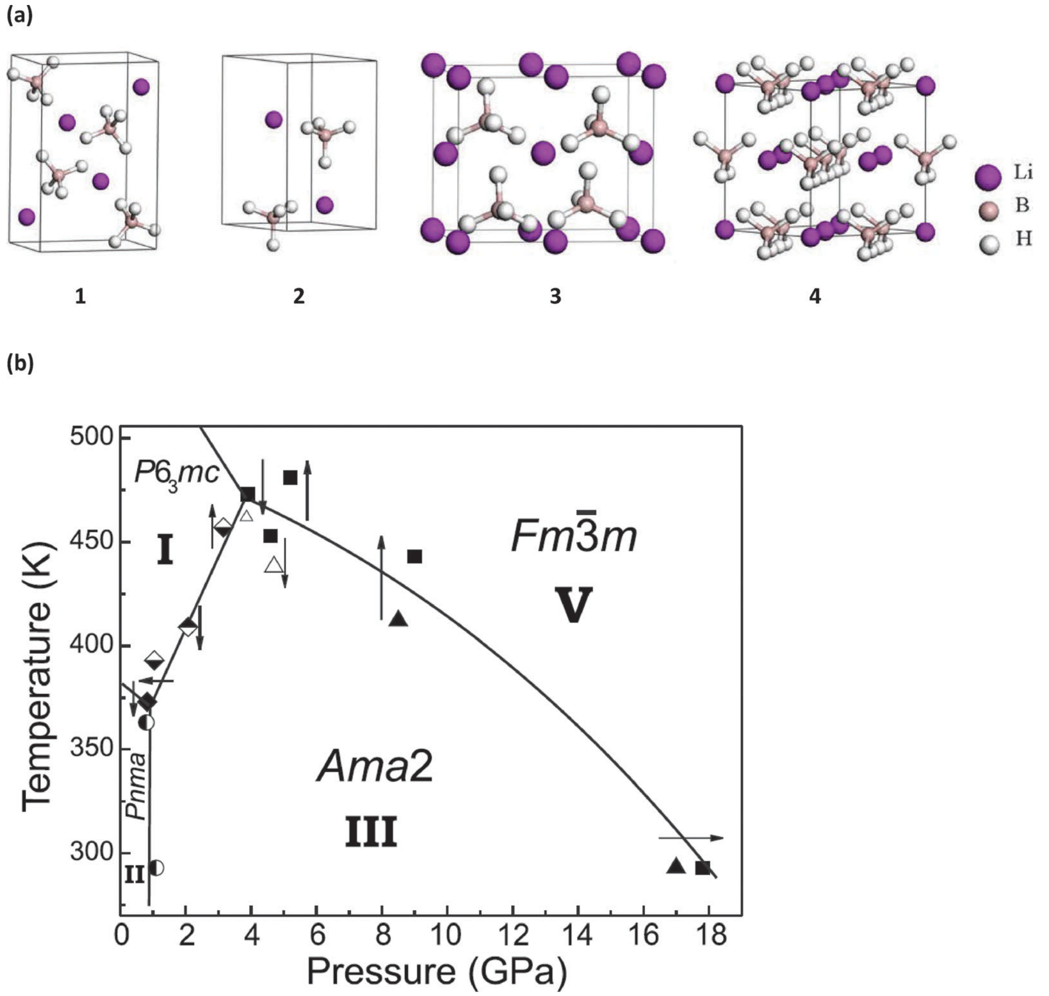

Fig. 3 (a) Crystal structures of $LiBH_4$. The space groups for different phases are: **1**: *Pnma* (α or II); **2**: $P6_3mc$ (I); **3**: *Ama*2 (β or III); **4**: $Fm\bar{3}m$ (V). Reproduced with permission.[115] Copyright 2011 International Association of Hydrogen Energy. (b) Pressure–temperature phase diagram of $LiBH_4$. Reproduced with permission.[120] Copyright 2008 American Physical Society.

first order phase transition to a hexagonal structure (space group $P6_3mc$, known as phase I, Fig. 3a, **2**) was observed as characterized by synchrotron X-ray powder and single crystal diffraction, where the $[BH_4^-]$ tetrahedron is believed to be more symmetric due to the rotational disorder.[116,117] Using Raman spectroscopy and X-ray diffraction, Talyzin *et al.*[118] observed a pressure-induced phase transition from α to β phase (or phase III) for $LiBH_4$ at a pressure of around 1 GPa, but the crystal structure of the β-phase was not determined. A further synchrotron experiment aided by first principles calculations allowed Filinchuk *et al.*[119] to determine the crystal structure of phase III to be an orthorhombic space group of *Ama*2 with a lower symmetry of distorted BH_4^- anions (Fig. 3a, **3**). In addition, a new high pressure phase was observed starting from 10 GPa. This phase was labeled phase V and identified with a cubic space group $Fm\bar{3}m$, a high symmetry lattice but with distorted BH_4^- anions (Fig. 3a, **4**). It is interesting to note that in each of the phases (I, II, and III), the Li^+ forms a tetrahedral, square-planar, and octahedral coordination, respectively, in response to compression. The same group of authors subsequently mapped out the phase diagram of $LiBH_4$ (Fig. 3b) by using *in situ* high-temperature (up to 500 K) and high pressure (up to 10 GPa) synchrotron measurements.[120] It is believed that the layered structures and deformations may influence the structural stabilities of its high pressure phases that in turn affect its hydrogen storage capabilities.[119] In addition, several theoretical calculations provide further insight into the high-pressure structures and stabilities of the known phases of $LiBH_4$ as well as other possible structures at high pressures.[121–124]

4.2 $NaBH_4$

Having a gravimetric hydrogen content of 10.6%, sodium borohydride ($NaBH_4$) is the most extensively studied of all borohydrides as a promising fuel source for the future hydrogen economy.[125–128] With a high decomposition temperature (*i.e.*, 673 K), $NaBH_4$ typically provides hydrogen *via* hydrolysis instead of through thermal activation, providing a remarkably high hydrogen yield (*i.e.*, ∼21 wt%):[128]

$$NaBH_4 + 2H_2O \rightarrow NaBO_2 + 4H_2 \qquad (5)$$

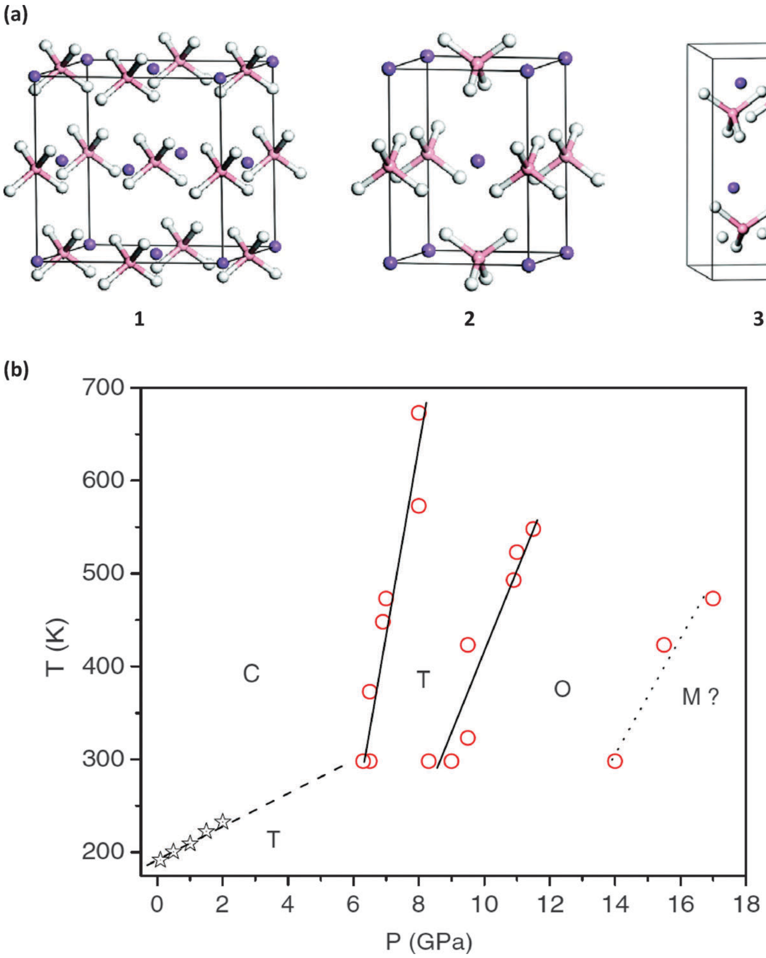

Fig. 4 (a) Crystal structures of $NaBH_4$. The space groups for different phases and presentation legends are: **1**: $Fm\bar{3}m$ (α phase); **2**: $P\bar{4}2_1c$ (β phase); **3**: *Pnma* (γ phase), purple: Na, pink: B and white: H. Reproduced with permission.[135] Copyright 2007 American Chemical Society. (b) Pressure–temperature phase diagram of $NaBH_4$. Reproduced with permission.[141] Copyright 2009 American Institute of Physics.

$NaBH_4$ crystallizes into a cubic structure (space group $Fm\bar{3}m$, known as the α phase) under ambient conditions (Fig. 4a, **1**).[129] Using Raman spectroscopy and thermal conductivity analysis, Sundqvist and Anderson[130] reported a low temperature phase below 190 K, which has a tetragonal structure of $P\bar{4}2_1c$ (known as β-$NaBH_4$, Fig. 4a, **2**).[131,132] Using Raman spectroscopy, Araújo *et al.* reported a pressure-induced phase transition at ∼10 GPa.[133] Using synchrotron X-ray diffraction, almost concurrently, Kumar and Cornelius investigated $NaBH_4$ up to 30 GPa.[134] It was found that α-$NaBH_4$ transforms to β-$NaBH_4$ at 6.3 GPa, indicating that the high pressure and the low temperature phases are identical. Further compression to 8.9 GPa resulted in the transition to an orthorhombic phase (space group *Pnma*) known as γ-$NaBH_4$. These observations were further confirmed by later X-ray and neutron diffraction and first principles calculations.[135] Using synchrotron powder diffraction aided by *ab initio* calculations, Filinchuk *et al.*[136] resolved the detailed crystal structure of γ-$NaBH_4$ as a $BaSO_4$-type structure (Fig. 4a, **3**). These structures were well reproduced by later density functional theory calculations.[137–140] Using *in situ* Raman spectroscopy and synchrotron X-ray diffraction, George *et al.* mapped the phase diagram of $NaBH_4$ at pressures of up to 17 GPa and temperatures of up to 673 K (Fig. 4b).[141]

4.3 KBH_4

Potassium borohydride (KBH_4) has a relatively high hydrogen content of 7.4 wt%, and, thus, has been investigated as a potential lightweight hydrogen storage material as well. Practically, it is often used in combination with other ''lighter'' metal hydrides in the bimetallic form for improved hydrogen content and storage performance.[142] KBH_4 crystallizes in the NaCl type cubic structure (space group $Fm\bar{3}m$), known as the α phase, under ambient conditions.[132,143] Using *in situ* Raman spectroscopy, and synchrotron X-ray diffraction aided by density functional calculations, Kumar *et al.*[144] investigated the high pressure behavior of KBH_4 up to 20 GPa. It was found that the α-KBH_4 phase transforms into tetragonal β-KBH_4 (space group $P\bar{4}2_1c$) at 3.8 GPa and then into the orthorhombic γ-KBH_4 phase (space group *Pnma*) at 6.8 GPa, which is similar to the phase transition sequence observed for the iso-structural $NaBH_4$ discussed earlier. The structures are thus identical to those of $NaBH_4$ (see Fig. 4a).

4.4 $Ca(BH_4)_2$

Among alkaline earth metal borohydrides, calcium borohydride [$Ca(BH_4)_2$] with a hydrogen content of 11.5 wt% has been most intensively investigated for hydrogen storage applications.[145–151] Although magnesium borohydride [$Mg(BH_4)_2$] has a high hydrogen content (*e.g.*, 14.8%), it has poor dehydrogenation–rehydrogentation kinetics. Instead, $Ca(BH_4)_2$ exhibits a highly reversible (de)hydrogenation ability *via* different reaction pathways, such as those illustrated below:[145,148,149,152]

$$Ca(BH_4)_2 \rightarrow CaH_2 + 2B + 3H_2 \quad (6)$$

$$3Ca(BH_4)_2 \rightarrow 2CaH_2 + CaB_6 + 10H_2 \quad (7)$$

$Ca(BH_4)_2$ has rich crystal polymorphs depending on the particular synthetic conditions. For instance, $Ca(BH_4)_2$ prepared by the desolvation of commercial $Ca(BH_4)_2{\cdot}2THF$ crystallizes into an α-phase with an orthorhombic structure (space group *Fddd* or *F*2*dd* shown in Fig. 5, **1** or **2**), which is believed to be the primary stable phase at both room and lower temperatures.[153] However, other space groups were also proposed later, making the structure of the α-phase $Ca(BH_4)_2$ still controversial.[154,155] Upon annealing to high temperature or by ball milling, the α-phase $Ca(BH_4)_2$ can be irreversibly transformed to a new

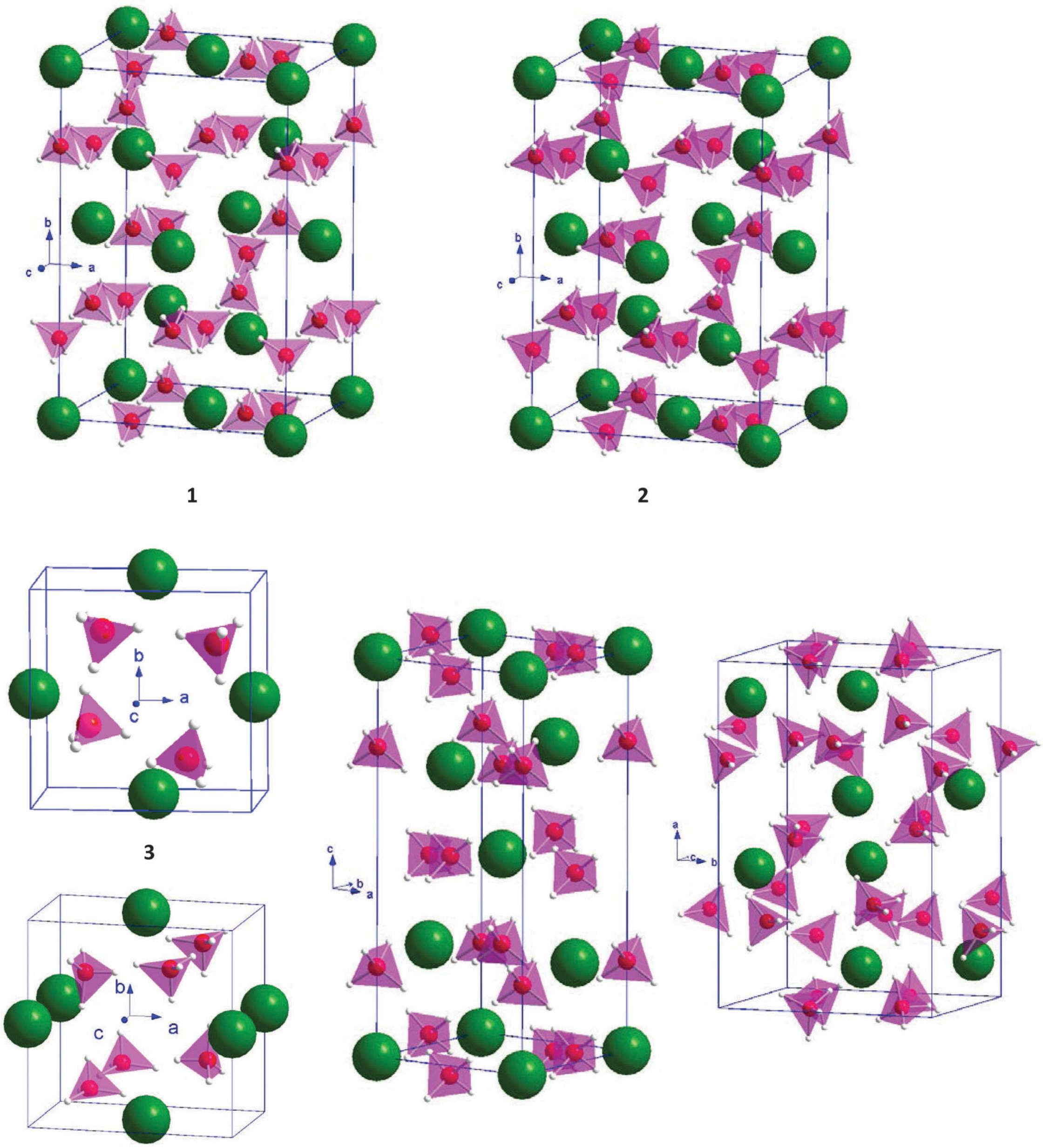

1 **2** **3** **4** **5** **6**

Fig. 5 Crystal structures of $Ca(BH_4)_2$. The space groups for different phases are: α phase, *Fddd* (**1**) or *F*2*dd* (**2**); β phase, $P\bar{4}$ (**3**) or $P4_2/m$ (**4**); γ phase, *Pbca* (**5**); α′ phase, $I\bar{4}2d$ (**6**). Atom colors: H: white; B: pink; Ca: green.

structure (labeled as the β-phase, Fig. 5, **3**).[155,156] Alternatively, the β-phase $Ca(BD_4)_2$ can be directly synthesized by a solid–gas reaction among MgB_2, CaD_2 and D_2 under high T–P conditions.[157] Similarly, although believed to have a tetragonal structure, the exact space group for β-phase $Ca(BH_4)_2$ (either $P\bar{4}$ or $P4_2/m$, Fig. 5, **3** or **4**) is also controversial.[154,155,158,159] Furthermore, during the heating process of α-$Ca(BH_4)_2$, additional polymorphs, *e.g.*, α′-$Ca(BH_4)_2$ (space group $I\bar{4}2d$, Fig. 5, **5**), γ-$Ca(BH_4)_2$ (space group *Pbca*, Fig. 5, **6**) and the σ phase, were also reported.[154,155,158,160] George *et al.*[161] conducted Raman and synchrotron X-ray diffraction studies on both α- and β-phase $Ca(BH_4)_2$ and found that the α-phase is stable under compression while β-$Ca(BH_4)_2$ transforms into a disordered structure above 10 GPa. Using combined Raman and IR spectroscopy, however, Liu *et al.*[162] reported several pressure-induced phase transitions for the α-phase $Ca(BH_4)_2$ and one of the high pressure phases may have a denser β-structure with the space group $P\bar{4}$ rather than with $P4_2/m$, consistent with the results from Majoub and Filinchuk.[154,155] Using density functional theories, infrared spectroscopy and inelastic neutron scattering, Borgschulte *et al.*[163] investigated the structural stabilities and thermodynamic properties of these polymorphs of $Ca(BH_4)_2$. Other polymorphs of $Ca(BH_4)_2$ have been computationally predicted but not experimentally observed.[164] A recent differential scanning calorimetric study suggests that the pure $Ca(BH_4)_2$ polymorphs have slightly different kinetic barriers and that their polymorphic content determines their decomposition kinetics.[165]

5. Amides

Amides $[M(NH_2)_x]$, or imides $[M(NH)_x]$, are a relatively new class of lightweight complex metal–nitrogen-hydrides of enormous interest for hydrogen storage,[166–168] inspired by the pioneering work of Chen *et al.* a decade ago.[169] Due to the relatively low hydrogen content as compared to other complex metal hydrides, most of the studies were made on lithium-based amides/imides.[170] In the following section, we review $LiNH_2$

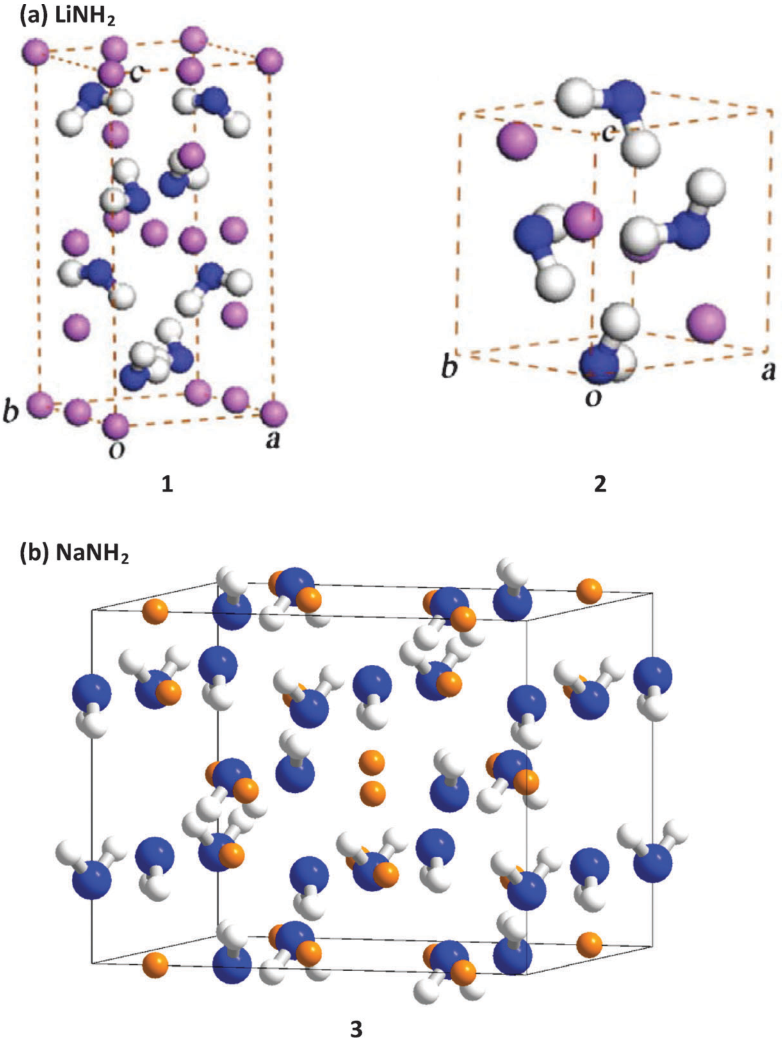

Fig. 6 Crystal structures of (a) $LiNH_2$ (**1**: space group $I\bar{4}$ (α phase) and **2**: space group $P2_1$ (β phase)), reproduced with permission.[172] Copyright 2012 American Chemical Society; and (b) $NaNH_2$ (**3**: space group *Fddd*). Atom colors: H: white; N: blue; Li: pink; Na: orange.

and $NaNH_2$, the only two amides that have been investigated at high pressures so far.

5.1 $LiNH_2$

Although containing only 8.8 wt% of hydrogen, lithium amide ($LiNH_2$) can be involved in the following reversible processes, yielding a high hydrogen content of 11.5% (per mole of Li_3N):[169]

$$Li_3N + 2H_2 \leftrightarrow Li_2NH + LiH + H_2 \leftrightarrow LiNH_2 + 2LiH \quad (8)$$

At temperatures below 573 K, $LiNH_2$ was observed to reversibly store ~6.5 wt% hydrogen during desorption and absorption following the reaction:[169]

$$LiNH_2 + LiH \leftrightarrow Li_2NH + H_2 \quad (9)$$

Under ambient conditions, $LiNH_2$ crystallizes into a tetragonal structure with space group $I\bar{4}$ (known as α-phase, Fig. 6a, **1**). Upon compression to ~12 GPa, Chelleppa *et al.* observed a reversible structural transition to a β phase as characterized by *in situ* Raman spectroscopy.[171] Very recently, using *in situ* synchrotron X-ray diffraction aided by first principles calculations, Huang *et al.*[172] resolved the structure of the high pressure β-$LiNH_2$ as a monoclinic $P2_1$ (Fig. 6a, **2**), which is 11% denser than the α phase. More recently, theoretical studies have predicted new high pressure structures for $LiNH_2$.[173]

5.2 $NaNH_2$

Although it has a lower hydrogen content (*i.e.*, 5.2%) than $LiNH_2$, sodium amide ($NaNH_2$) can still play an important role in facilitating hydrogen release when used in conjunction with other metal hydrides (*e.g.* $LiAlH_4$ or MgH_2) by forming intermediate hydride complexes.[174,175] $NaNH_2$ crystallizes into an orthorhombic cell under ambient conditions with space group *Fddd* (Fig. 6b). Using combined *in situ* Raman and infrared absorption spectroscopy, Liu and Song observed two reversible pressure-induced phase transitions at 0.9 and 2.0 GPa, respectively.[176] The high pressure phase is believed to be disordered or amorphous. No X-ray diffraction data are currently available to resolve the high pressure structures, although a recent computational work predicted new high pressure structures for $NaNH_2$.[177]

6. Chemical hydrides

Similar to complex metal hydrides, chemical hydrides also contain a large capacity of hydrogen. The difference is that this class of materials does not contain metal elements and, thus, is a covalent compound in nature. As a result, chemical hydrides are typically used as one-way hydrogen storage materials with only dehydrogenation processes. The representative materials in this category are diborane and ammonia borane.

6.1 B_2H_6

Diborane (B_2H_6) is the simplest stable boron hydride with an extremely high hydrogen content of ~22%. Compared to other hydrides, it has a very low decomposition temperature with positive heat of formation, so the dehydrogenation is readily spontaneous due to its thermodynamic instability. Despite these desirable properties, however, diborane by itself has not been attempted as a hydrogen storage material from technical perspective because of the cost and other safety issues. Instead, it has been most studied because of its peculiar structural chemistry.[178] Due to the electron deficiency, for example, it has hydrogen bridge bonds that are found only in the borane family. Especially at high pressures, it has been predicted to transform into a stable phase with a structure of a very high hydrogen density, making the application for hydrogen storage an interesting possibility.[179]

Under ambient conditions, diborane is a flammable gas and solidifies at 108 K. At ambient pressure and below 60 K, solid diborane crystallizes into the α phase with an orthorhombic structure, while annealing to above 90 K results in the formation of the β phase (space group $P2_1/n$, Fig. 7a). Using Raman and infrared absorption spectroscopy, Murli and Song investigated the high pressure structures of diborane up to 50 GPa at room temperature.[180,181] A liquid to solid transition was observed at ~4 GPa. Further compression resulted in the formation of two additional solid phases at around 7 and 14 Gpa, respectively, as evidenced by the different characteristic modes occurring across these boundaries. However, the high pressure crystal structures have not been characterized by X-ray diffraction. A recent simulation work indicated that the high pressure phase I is identical to the low-temperature phase, β-B_2H_6.[182] Other interesting high pressure structures of B_2H_6 were also predicted, but no new experimental data are available so far.[183,184]

6.2 NH_3BH_3

Ammonia borane (NH_3BH_3) contains over 19 wt% H_2 and 150 g H_2 per L and has been studied and reviewed extensively for on-board hydrogen storage applications.[185–191] At room temperature and under ambient pressure, NH_3BH_3 is a stable solid. Hydrogen can be released by heating NH_3BH_3 to temperatures ranging from 350 K to 410 K, yielding polyaminoborane $(BH_2NH_2)_x$ exothermically; continued heating results in the release of a second equivalent hydrogen at temperatures from 380 K to 470 K, yielding polyiminoborene $(BHNH)_x$ and borazine $(B_3N_3H_6)$:[189]

$$H_3N\text{–}BH_3 \rightarrow 1/x\ (H_2N\text{–}BH_2)_x + H_2 \quad (10)$$

$$(H_2N\text{–}BH_2)x \rightarrow 1/x\ (HN\text{–}BH)_x + H_2 \quad (11)$$

$$1/x\ (HN\text{–}BH)_x \rightarrow BN + H_2 \quad (12)$$

Because of the slow kinetics, however, a catalyzed dehydrogenation mechanism, or hybridization with other metal hydrides,[192–194] or other ammonia borane derivatives (*e.g.*, $LiNH_2BH_3$ and $NaNH_2BH_3$), is being developed for practical hydrogen storage applications.[195]

At room temperature, NH_3BH_3 adopts a tetragonal structure with the space group *I4mm* (Fig. 7b, **2**).[196,197] This molecular crystal undergoes a phase transition from an orientationally

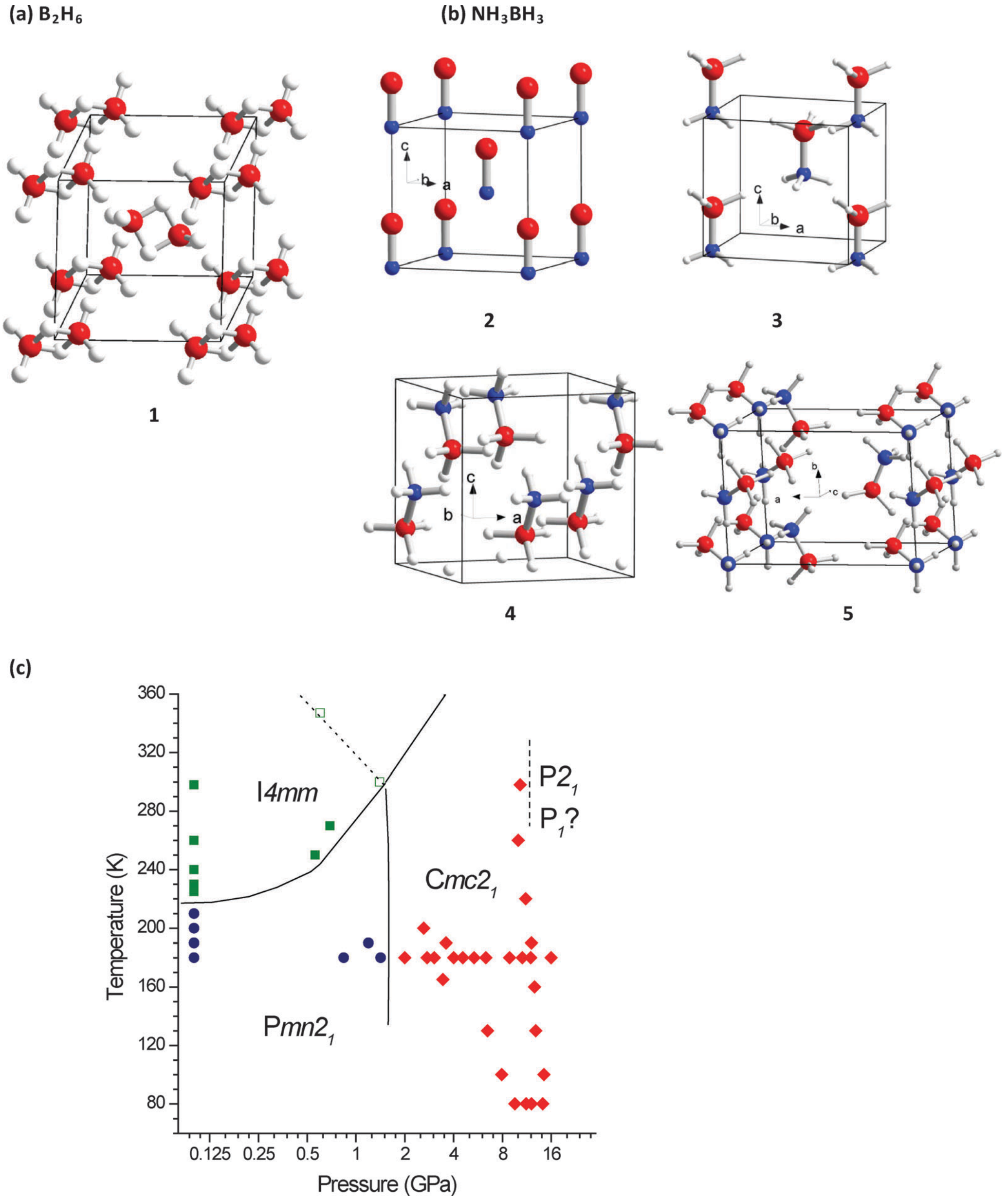

Fig. 7 Crystal structures of (a) B_2H_6 (**1**: space group $P2_1/n$ (β phase)); and (b) NH_3BH_3 (**2**: space group $I4mm$; **3**: space group $Pmn2_1$; **4**: space group $Cmc2_1$; and **5**: space group $P2_1$), partially reproduced from ref. 214 with permission. Copyright 2012 American Chemical Society. Atom colors: H: white; B: red; N: blue. (c) Pressure–temperature phase diagram of NH_3BH_3 modified from ref. 214 using the updated information from ref. 212 and 215.

disordered tetragonal phase to an orthorhombic structure when cooled to 225 K,[198] resulting in a significant change in the lattice dynamics.[199–202] However, the molecular structure of the NH_3BH_3 molecule is preserved. This orthorhombic structure was shown to have the space group $Pmn2_1$ (Fig. 7b, **3**).[196,203] Early spectroscopy studies have demonstrated that NH_3BH_3 undergoes two phase transitions upon compression to 4 GPa.[204,205] Later, Lin *et al.*[206] and Xie *et al.*[207] performed independent high-pressure studies on ammonia borane up to 20 GPa using Raman spectroscopy and combined Raman/IR spectroscopy, respectively, and similar new phase transitions were found in the higher pressure regions in both studies. The crystal structures of these new high-pressure phases were subsequently examined by X-ray diffraction measurements and theoretical calculations by Filinchuk *et al.*[208] and Chen *et al.*[209] They consistently established that at room temperature and above 1.5 GPa, NH_3BH_3 crystallizes into a new ordered orthorhombic structure (space group $Cmc2_1$, Fig. 7b, **4**). Further high-pressure X-ray and neutron diffraction experiments and density functional calculations confirmed these observations, but also proposed a new triclinic structure with a space group of $P1$ above 8 GPa.[210] Most recently, Wang *et al.*[211] investigated the structural and dynamical properties of ammonia borane at high pressures up to 60 GPa using molecular dynamics simulations, which helped with the understanding of the relationship and the transformation mechanisms among the three known phases of ammonia borane. The phase boundaries of NH_3BH_3 were established in the pressure region of 0–1.5 GPa and the temperature region of 110–300 K by Andersson *et al.*[212] using thermal conductivity measurements, and by Najiba *et al.*[213] using Raman spectroscopy, respectively. Using *in situ* low-temperature Raman spectroscopy, Liu and Song have mapped the phase diagram of NH_3BH_3 in an extended temperature range of 80 to 350 K and a pressure range of 0 to 15 GPa.[214] Concurrently, Lin *et al.*[215] reported a new high-pressure phase of NH_3BH_3 (space group $P2_1$, Fig 7b, **5**) at above 12.9 GPa as characterized by *in situ* synchrotron X-ray powder diffraction aided by density functional calculations. A more recent high-pressure Raman study up to 65 GPa suggested a new phase transition at 27 GPa.[216] All of this new information has allowed the updating of the phase diagram of NH_3BH_3 as shown in Fig. 7c.

7. Hydrogen-containing complexes

Hydrogen storage in molecular systems is a relatively new and alternative approach that stems from the discovery of the formation of novel hydrogen-containing complexes under high pressure conditions. These complexes are typically super-molecular compounds, or clathrate materials, with guest–host structures, where host molecules form inclusional cages or some other framework structures, and hydrogen was either enclosed or stored as a guest molecule.[217–219] The distances between the host and the guest molecules are typically in the order of van der Waals interactions, implying that no conventional chemical bonds were formed between the host and guest. It was found that pressure can serve as an effective driving force to facilitate the formation of novel complexes between hydrogen and other simple molecules, such as CH_4, NH_3, H_2O and even noble gases. Many of these host molecules are already hydrogen rich and thus have been used as hydrogen sources themselves (*e.g.*, CH_4 and H_2O). Without the limitations of conventional stoichiometry, these complexes can store an enormous amount of additional hydrogen, far exceeding the US DOE target. In addition, once formed at high pressures, hydrogen can often be spontaneously released under near ambient pressure/temperature conditions, a very desirable property for practical hydrogen storage applications. In the following section, we review those complexes that have been observed and characterized under high pressures to date.[220]

7.1 CH_4–H_2

In 1996, Somayazulu *et al.*[221] first reported pressure-induced chemistry in the CH_4–H_2 system observed in diamond anvil cells using Raman spectroscopy and synchrotron crystallography. The binary system CH_4–H_2 was found to form four molecular compounds, $CH_4(H_2)_2$, $(CH_4)_2H_2$, $CH_4(H_2)_4$, and CH_4H_2, at pressures up to 10 GPa. Among these novel compounds, $CH_4(H_2)_4$ holds a remarkable 33.4 wt% H_2 (and a total of 50 mass% H). The crystal structure of this hydrogen rich complex was preliminarily identified as a body-centered tetragonal lattice, but no detailed space group was reported. $CH_4(H_2)_4$ can readily transform into the next hydrogen rich complex, $CH_4(H_2)_2$ upon compression and the crystal structure for $CH_4(H_2)_2$ has been determined to be a hexagonal $MgZn_2$ structure with a space group of $P6_3/mmc$ (Fig. 8 inset). The stoichiometry and transformations of these compounds were subsequently examined as a function of pressure by X-ray, infrared and Raman studies conducted by the same group.[222] The pressure–composition phase diagram is shown in Fig. 8. Mao *et al.*[223] subsequently examined the melting curve for $CH_4(H_2)_4$ with an attempt to recover the material under ambient conditions. It was found that $CH_4(H_2)_4$ can be quenched at an ambient pressure and a temperature of 10 K, and that it decomposes at approximately 23 K. A more recent *ab initio* study on $CH_4(H_2)_4$ attempting to recover the material suggests that it's possible to produce the complex through external agents such as MOF materials and carbon nanotubes.[224]

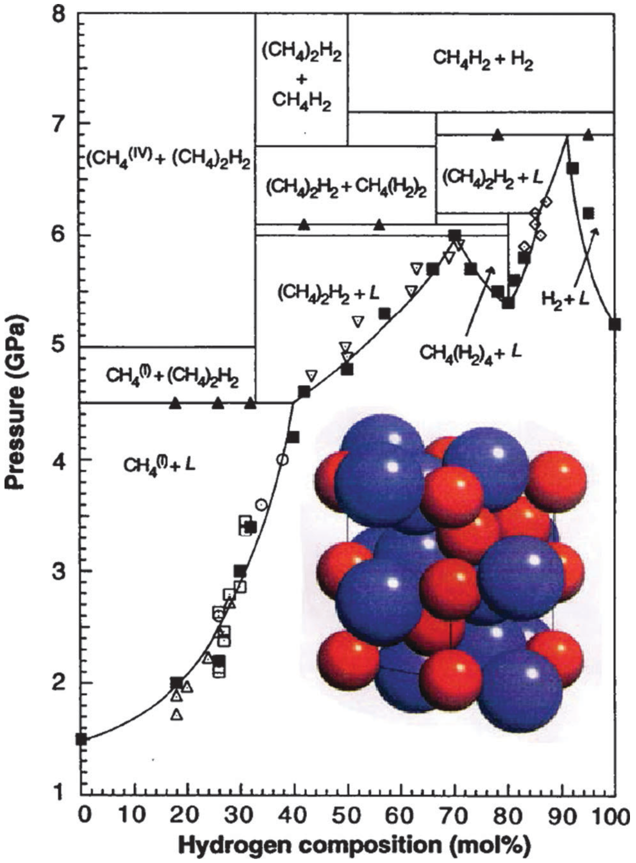

Fig. 8 Pressure–mole fraction diagram of the binary molecular system CH_4–H_2 at 298 K. Inset: crystal structures of $CH_4(H_2)_2$ compound (space group $P6_3/mmc$), blue balls denote CH_4 molecules and red balls denote H_2. Reproduced with permission.[221] Copyright 1996 AAAS.

7.2 H_2O–H_2

As mentioned earlier, a hydrogen–water complex in the form of clathrate hydrate has emerged as a new and promising hydrogen storage material[217–219,225–228] and has, thus, undergone extensive investigation. In 1993, Vos *et al.*[229] first reported the formation of two types of H_2O–H_2 complexes in the form of filled ice or hydrogen clathrates under high pressures as characterized by X-ray diffraction and Raman spectroscopy. A C_1 (clathrate 1) structure that contains 36 water molecules hosting 6 hydrogen molecules (*i.e.*, $H_2O:H_2 = 6:1$) in a unit cell was formed at $\sim$0.7 GPa and room temperature. This C_1 phase adopts the trigonal crystal structure of ice II (space group $R\bar{3}$) with ordered protons (Fig. 9a, **1**). The compression of the C_1 phase above 2.3 GPa resulted in the formation of a C_2 phase with a cubic diamond structure (space group $Fd\bar{3}m$, Fig. 9a, **2**) with 8 water molecules and 8 hydrogen molecules in the unit cell ($H_2O:H_2 = 1:1$). The C_2 structure is stable up to at least 30 GPa.[229,230] In 2002, Mao *et al.*[46] discovered a third type of hydrogen clathrate,

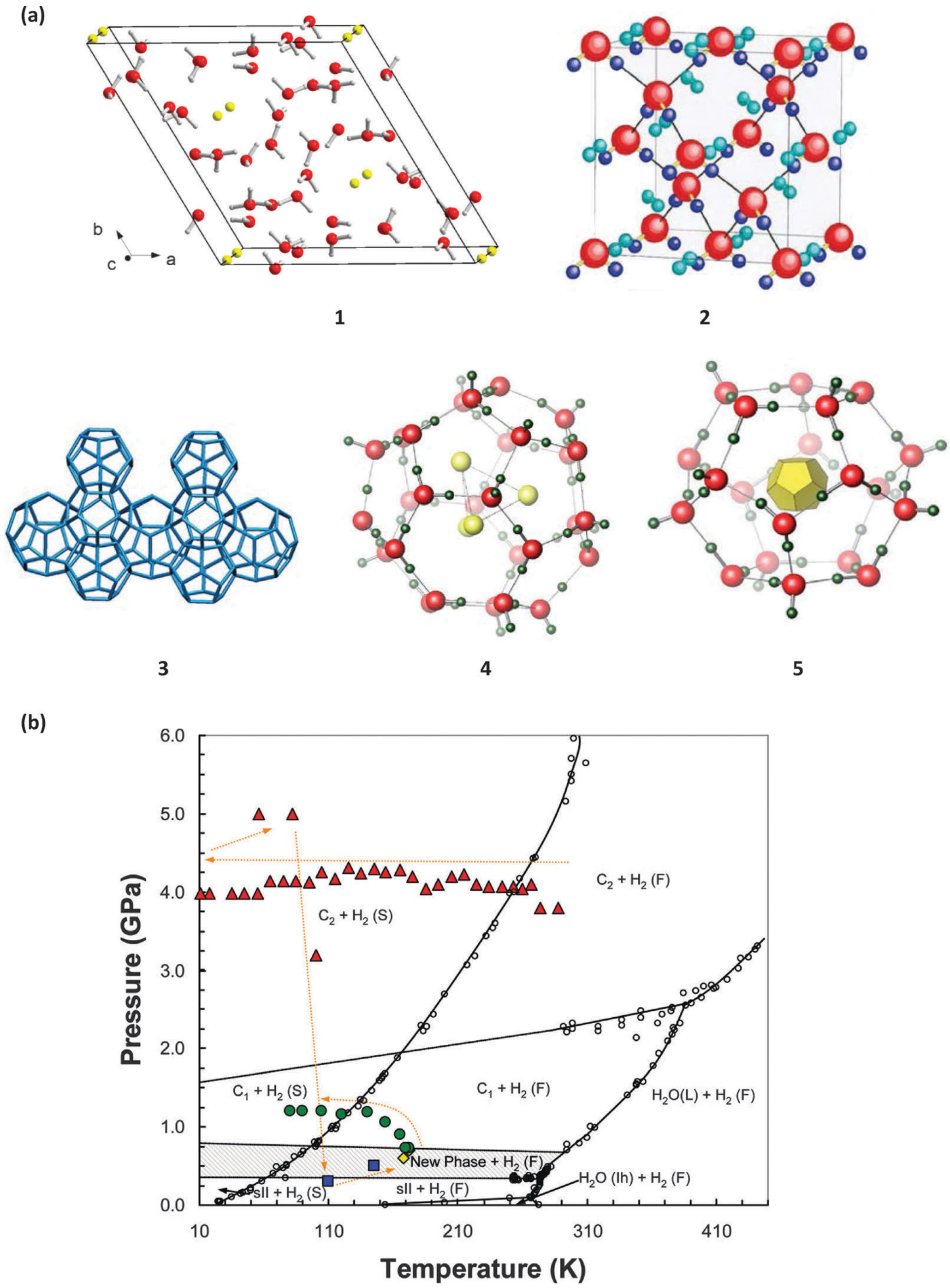

Fig. 9 (a) Structures of known hydrogen clathrate hydrates. **1**: Crystal structure of Clathrate 1 (C_1), space group $R\bar{3}$; red and white balls are oxygen and hydrogen atoms in water molecules while the yellow balls denote positions for H_2 with no specific orientation; **2**: Crystal structure of Clathrate 2 (C_2), space group $Fd\bar{3}m$; **3–5**: Structure of clathrate sII. **3**: Polyhedral representation of the large and small cages. Reproduced with permission.[237] Copyright 2009 American Chemical Society; **4**: The large cage with four encaged hydrogen molecules; and **5**: The small cage with two encaged hydrogen molecules. Reproduced with permission.[231] Copyright 2004 American Physical Society. (b) Pressure–temperature phase diagram of H_2O–H_2 system. Reproduced with permission.[251] Copyright 2011 American Chemical Society.

called structure two (sII) clathrate hydrate, when the H_2O–H_2 mixture was compressed to 180–220 MPa and cooled down to <250 K. The sII clathrate hydrate adopts a cubic structure with a space group of $Fd\bar{3}m$. And the unit cell contains a total of 136 water molecules and 48 hydrogen molecules in two types of arrangements: one with 4 hydrogen molecules in each of the eight hexakiadecahedrals ($5^{12}6^4$) and one with 2 hydrogen molecules in each of the sixteen pentagonal dodecahedrals (5^{12}) as shown in Fig. 9a, **3–5**.[231] This novel clathrate can be recovered by pressure-quenching and is stable up to 145 K at an ambient pressure, shedding light on practical hydrogen storage applications. Since then, the structures, stability, transitions, production, dynamics, and kinetics involving C_1, C_2, sII clathrates and other possible hydrogen clathrates have been extensively characterized by spectroscopy, X-ray and neutron diffractions and first principle calculations in a broader pressure and temperature range.[232–247] As a result, the pressure–temperature phase diagram of the H_2–H_2O system is now relatively well established.[248–251] Fig. 9b shows the structure and stability phase diagram of all the known hydrogen clathrate hydrates, which has recently been updated by Strobel *et al.*[251]

7.3 SiH_4–H_2 and GeH_4–H_2

Silane (SiH_4) has been under extensive experimental and theoretical investigation due to its predicted and observed peculiar high-pressure structures, and its optical and electronic properties with implications for metallization.[252–255] In 2009, Strobel *et al.*[256] and Wang *et al.*[257] almost concurrently reported the observation of novel SiH_4–H_2 complexes. Above 7 GPa, in particular, Strobel observed the formation of a novel hydrogen-rich solid in the form of $SiH_4(H_2)_2$. The synchrotron power X-ray diffraction revealed the crystal structure of such a complex to be cubic $F\bar{4}3m$ (Fig. 10a). It is especially interesting to note the unusual interactions between SiH_4 and H_2 molecules with important implications of pressure-induced perturbation and destabilization of the H–H covalent bond at relatively low pressures. Using Raman spectroscopy, Wang *et al.* observed the consistent high pressure behavior of SiH_4–H_2 and established that SiH_4–H_2 fluid shows a binary eutectic point at 72 mol% H_2 and 6.1 GPa, above which the fluid crystallizes into a mixture of two nearly end-member solids, which may be regarded as doped hydrogen dominant compounds. Similar SiH_4–H_2 phase diagrams constructed in both studies with that made by Strobel *et al.* are shown in Fig 10b. Subsequent first principles calculations to elucidate the electronic structures and chemical bonding for $SiH_4(H_2)_2$ were also reported extensively.[258–266]

In 2010, Strobel *et al.* reported the formation of a similar complex formed between germane (GeH_4) and hydrogen.[267] Using optical microscopy, Raman and IR spectroscopy as well as synchrotron diffraction, a new molecular complex with an approximate stoichiometry of $GeH_4(H_2)_2$ and a cubic crystal structure[268] was characterized above 7.5 GPa. However, the complex became unstable above 17 GPa due to decomposition. A follow-up computational work investigated the structural, electronic and dynamic properties of this complex with the prediction of new high pressure structures.[269] Although silane and germane may not have significant potential for hydrogen storage, from a practical point of view due to cost and safety issues, their unusual bonding mechanisms and covalent bond destabilizations have important implications for the development of hydrogen-rich, molecular-based storage materials.

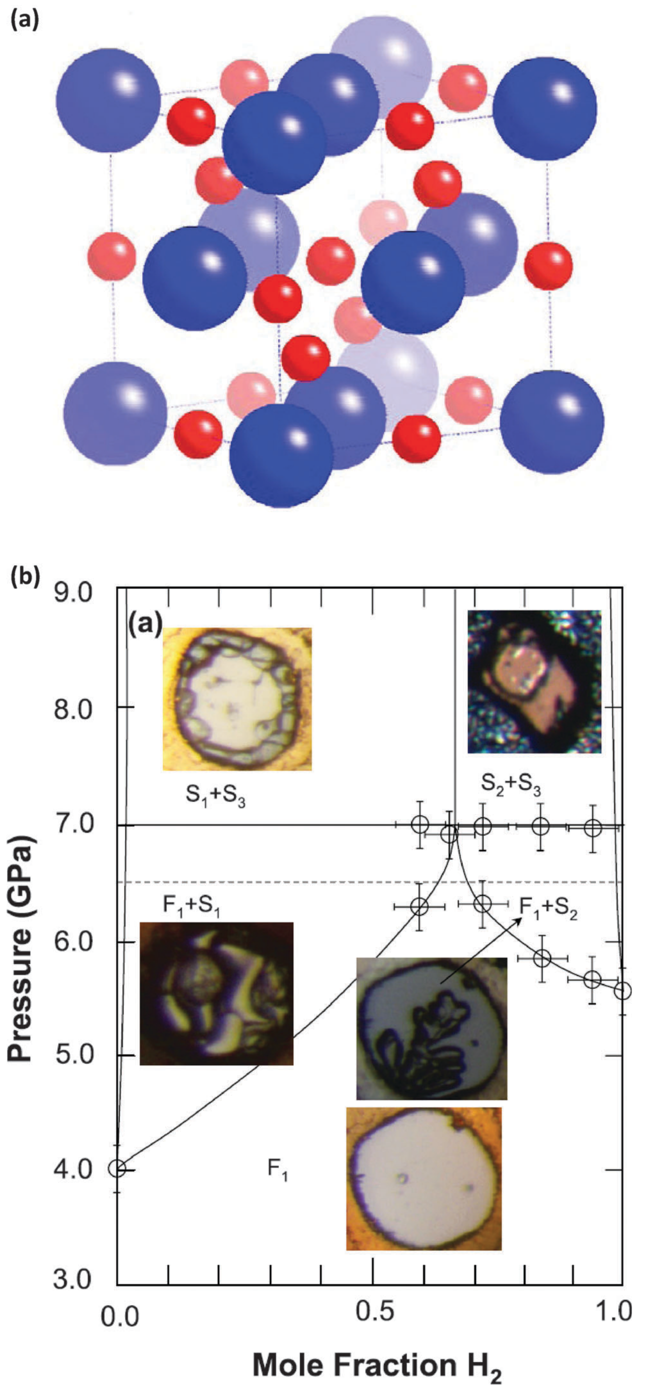

Fig. 10 (a) Crystal structure of $SiH_4(H_2)_2$ (space group $F\bar{4}3m$). The blue and red balls denote SiH_4 and H_2 molecules respectively. (b) Pressure–mole fraction diagram of the SiH_4–H_2 binary system. Reproduced with permission.[256] Copyright 2009 American Physical Society.

7.4 NH_3BH_3–H_2

As discussed above, ammonia borane (NH_3BH_3) has been extensively investigated under high pressures as a promising hydrogen storage material by itself. In 2009, Lin *et al.*[270] discovered a novel solid phase of NH_3BH_3 in excess of molecular hydrogen at above 6.2 GPa by using optical microscopy and Raman spectroscopy. This phase has a stoichiometry of $NH_3BH_3(H_2)_x$, where $x \approx 1.3$–2, indicating 8–12 wt% of additional H_2. Considering the amount of H_2 already stored in the NH_3BH_3 molecule, this new and unique complex represents one of the most H_2-rich materials (with ~30 wt% H_2). Using *in situ* Raman spectroscopy, Wang *et al.* subsequently investigated the bonding interactions between molecular hydrogen and single crystal NH_3BH_3 under simultaneous high-pressure and high-temperature conditions.[271] The complex reaction kinetics, the bonding variations, and the slow reaction rates provided additional clues for designing new complexes for practical hydrogen storage applications. Almost concurrently, Chelleppa *et al.* reported a pressure-induced interaction of the NH_3BH_3–H_2 system up to 60 GPa using Raman spectroscopy.[272] The formation of two complexes at 6.7 GPa and 10 GPa was observed and additional structural, dynamic and kinetic information about the complex was discussed.

7.5 Ar–H_2 and Xe–H_2

Noble gas elements with closed electronic structures are considered inert under ambient conditions but can exhibit significantly different reactivities at high pressures, even with hydrogen. Originally driven by the pursuit of metallic hydrogen,[273] for example, the argon–hydrogen mixture was studied up to 175 GPa by Loubeyre *et al.* in 1994.[274] Using optical microscopy, Raman spectroscopy and synchrotron single crystal X-ray diffraction, a new stoichiometric complex $Ar(H_2)_2$ was observed at 4.3 GPa. This complex has a C14 Laves structure (isomorphous to $MgZn_2$) with space group $P6_3/mmc$ (Fig. 11a). The structure and stability of this complex have been subsequently investigated extensively at low temperatures down to 30 K by Raman and infrared measurements,[275–280] and up to 250 GPa by theoretical calculations.[281–284]

Similarly, xenon was also found to exhibit an enhanced interaction with hydrogen under compression. Using optical microscopy and Raman scattering, Jephcoat *et al.*[285] observed the formation of a stoichiometric phase of solid Xe–H_2 at 5.3 GPa from a 7.5 vol% Xe–H_2 mixture. In 2010, Somayazulu *et al.*[286] obtained the Xe–H_2 single crystal at 4.9 GPa and subsequently characterized its structure by optical spectroscopy and X-ray diffraction. This unique hydrogen-rich complex is estimated to have a stoichiometry of $Xe(H_2)_7$ in a hexagonal crystal structure (space group $R3$) that can be viewed as a tripled solid hydrogen lattice modulated by layers of xenon (Fig. 11b). In a follow-up *ab initio* calculation, Kaewmaraya *et al.*[287] attempted to provide an additional understanding of the electronic and bonding properties of such a complex. Once again, from the practical hydrogen storage perspective, although noble gas is not desirable due to the cost and extreme conditions required, the usual bonding properties and novel reactivities under high pressure may provide clues for the development of new hydrogen storage materials.

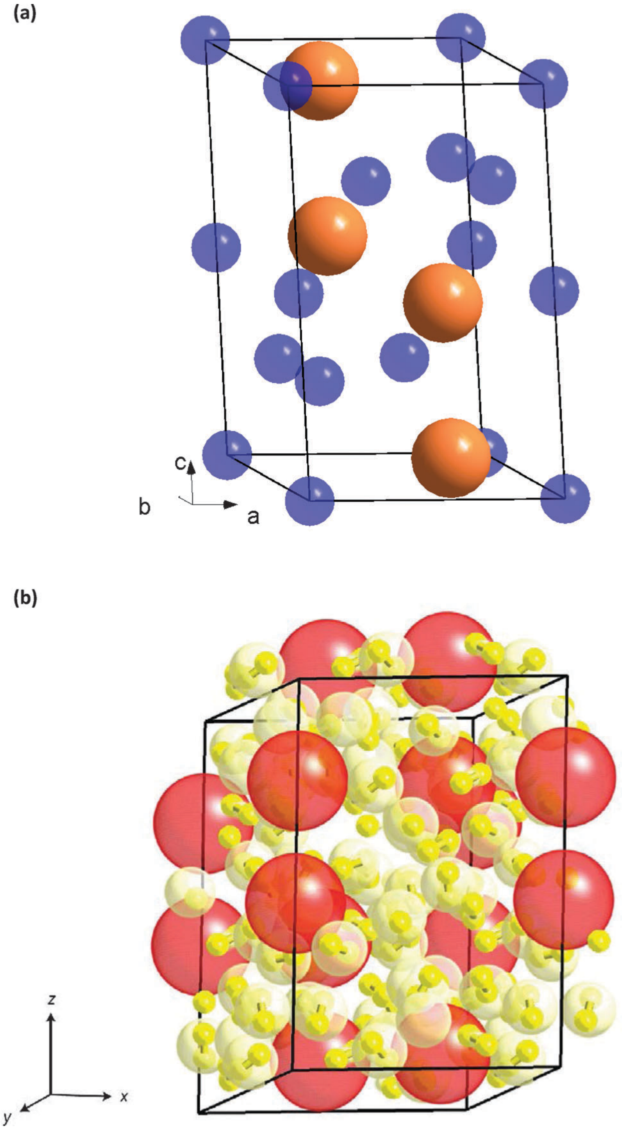

Fig. 11 (a) Crystal structure of $Ar(H_2)_2$ (space group $P6_3/mmc$). The orange and blue balls denote Ar atoms and H_2 molecules respectively; (b) Crystal structure of $Xe(H_2)_7$ (space group $R3$). Reproduced with permission.[286] Copyright 2010 Nature Publishing Group.

8. Conclusions and outlook

In this perspective article, we have reviewed a wide range of the most representative hydrides as promising hydrogen storage materials investigated under high pressures in recent years. The new structures, the enhanced hydrogen content, and the novel stoichiometry of hydrogen complexes demonstrate great promise for hydrogen storage application for these materials. Pressure as a simple and yet effective driving force has emerged as an alternative approach to developing new potential hydrogen storage materials. Understanding the structures and stabilities as well as the thermodynamic and kinetic properties of these materials, such as those of individual hydrides in various categories reviewed in this article, is of fundamental importance, and constitutes the first step in utilizing high-pressure to develop new materials with hydrogen storage potential and/or to enhance hydrogen storage capacity. The novel structures and phases discovered under high pressures, as well as the pressure-dependent electronic and bonding properties have provided key information on the (de)hydrogenation mechanisms and, thus, have important implications for enhancing hydrogen storage performance. The extensive and increasing research effort on the high-pressure study of potential hydrogen storage materials represents an exciting long-term research frontier.

For practical applications, it would be desirable to retrieve the novel hydrogen-rich systems once they are produced under extreme pressure or temperature conditions. Ideally, the formation pressures and temperatures used should be close to ambient conditions for practical bulk industrial production. To achieve this goal, the structures and the hydrogen storage/release properties need to be systematically investigated under an extended array of pressure–temperature conditions. Some new emerging hybrid hydrides (*e.g.*, $LiNH_2BH_3$ and $NaNH_2BH_3$)[195] that have rarely been investigated at high pressures may allow hydrogen storage and release under milder conditions and with more efficiency. In addition, more complicated systems such as the three-component system ($A–B–H_2$), where A is the hydrogen storage host, and B is the "catalyst" that may help to stabilize the formation of the new complex both at high pressures and under near ambient conditions,[288,289] could open a new avenue for the high-pressure development of hydrogen storage materials. Finally, more rational theoretical calculations are needed to assist with the prediction and design of novel hydrogen storage materials under high pressure conditions.

Acknowledgements

This work was supported by a Discovery Grant, a Research Tools and Instruments Grant from the Natural Science and Engineering Research Council of Canada, a Leaders Opportunity Fund from the Canadian Foundation for Innovation, and an Early Researcher Award from the Ontario Ministry of Research and Innovation.

References

1 L. Schlapbach, *Nature*, 2009, **460**, 809–811.
2 L. Schlapbach and A. Zuttel, *Nature*, 2001, **414**, 353–358.
3 http://www1.eere.energy.gov/hydrogenandfuelcells/storage/pdfs/targets_onboard_hydro_storage.pdf.
4 D. P. Broom, *Hydrogen Storage Materials*, Springer-Verlag London Limited, 2011.
5 W. Grochala and P. P. Edwards, *Chem. Rev.*, 2004, **104**, 1283–1315.
6 D. Chandra, J. J. Reilly and R. Chellappa, *JOM*, 2006, **58**, 26–32.
7 S. I. Orimo, Y. Nakamori, J. R. Eliseo, A. Zuttel and C. M. Jensen, *Chem. Rev.*, 2007, **107**, 4111–4132.
8 L. George and S. K. Saxena, *Int. J. Hydrogen Energy*, 2010, **35**, 5454–5470.
9 I. P. Jain, P. Jain and A. Jain, *J. Alloys Compd.*, 2010, **503**, 303–339.
10 J. Yang, A. Sudik, C. Wolverton and D. J. Siegel, *Chem. Soc. Rev.*, 2010, **39**, 656–675.
11 M. T. Kelly, *Fuel Cells and Hydrogen Storage*, Springer, New York, 2011, vol. 141, pp. 169–201.
12 R. J. Hemley, *Annu. Rev. Phys. Chem.*, 2000, **51**, 763–800.
13 W. Grochala, R. Hoffmann, J. Feng and N. W. Ashcroft, *Angew. Chem., Int. Ed.*, 2007, **46**, 3620–3642.
14 H. K. Mao and R. J. Hemley, *Rev. Mod. Phys.*, 1994, **66**, 671–692.
15 J. M. McMahon, M. A. Morales, C. Pierleoni and D. M. Ceperley, *Rev. Mod. Phys.*, 2012, **84**, 1607–1653.
16 N. W. Ashcroft, *Phys. Rev. Lett.*, 1968, **21**, 1748–1749.
17 K. A. Johnson and N. W. Ashcroft, *Nature*, 2000, **403**, 632–635.
18 E. Babaev, A. Sudbo and N. W. Ashcroft, *Nature*, 2004, **431**, 666–668.
19 S. A. Bonev, E. Schwegler, T. Ogitsu and G. Galli, *Nature*, 2004, **431**, 669–672.
20 R. J. Hemley and H. K. Mao, *Phys. Rev. Lett.*, 1988, **61**, 857–860.
21 H. K. Mao and R. J. Hemley, *Science*, 1989, **244**, 1462–1465.
22 M. Hanfland, R. J. Hemley and H. K. Mao, *Phys. Rev. Lett.*, 1993, **70**, 3760–3763.
23 R. J. Hemley, Z. G. Soos, M. Hanfland and H. K. Mao, *Nature*, 1994, **369**, 384–387.
24 N. H. Chen, E. Sterer and I. F. Silvera, *Phys. Rev. Lett.*, 1996, **76**, 1663–1666.
25 R. J. Hemley, H. K. Mao, A. Goncharov, M. Hanfland and V. Struzhkin, *Phys. Rev. Lett.*, 1996, **76**, 1667–1670.
26 P. Loubeyre, R. LeToullec, D. Hausermann, M. Hanfland, R. J. Hemley, H. K. Mao and L. W. Finger, *Nature*, 1996, **383**, 702–704.
27 S. T. Weir, A. C. Mitchell and W. J. Nellis, *Phys. Rev. Lett.*, 1996, **76**, 1860–1863.
28 B. Edwards and N. W. Ashcroft, *Nature*, 1997, **388**, 652–655.
29 C. Narayana, H. Luo, J. Orloff and A. L. Ruoff, *Nature*, 1998, **393**, 46–49.
30 A. F. Goncharov, E. Gregoryanz, R. J. Hemley and H. K. Mao, *Proc. Natl. Acad. Sci. U. S. A.*, 2001, **98**, 14234–14237.
31 P. Loubeyre, F. Occelli and R. LeToullec, *Nature*, 2002, **416**, 613–617.
32 E. Gregoryanz, A. F. Goncharov, K. Matsuishi, H. Mao and R. J. Hemley, *Phys. Rev. Lett.*, 2003, **90**, 175701.
33 S. Scandolo, *Proc. Natl. Acad. Sci. U. S. A.*, 2003, **100**, 3051–3053.
34 B. Edwards and N. W. Ashcroft, *Proc. Natl. Acad. Sci. U. S. A.*, 2004, **101**, 4013–4018.
35 C. J. Pickard and R. J. Needs, *Nat. Phys.*, 2007, **3**, 473–476.
36 P. Cudazzo, G. Profeta, A. Sanna, A. Floris, A. Continenza, S. Massidda and E. K. U. Gross, *Phys. Rev. Lett.*, 2008, **100**, 257001.

37 M. A. Morales, C. Pierleoni, E. Schwegler and D. M. Ceperley, *Proc. Natl. Acad. Sci. U. S. A.*, 2010, **107**, 12799–12803.

38 I. Tamblyn and S. A. Bonev, *Phys. Rev. Lett.*, 2010, **104**, 065702.

39 M. I. Eremets and I. A. Troyan, *Nat. Mater.*, 2011, **10**, 927–931.

40 N. Subramanian, A. F. Goncharov, V. V. Struzhkin, M. Somayazulu and R. J. Hemley, *Proc. Natl. Acad. Sci. U. S. A.*, 2011, **108**, 6014–6019.

41 R. T. Howie, C. L. Guillaume, T. Scheler, A. F. Goncharov and E. Gregoryanz, *Phys. Rev. Lett.*, 2012, **108**, 125501.

42 S. Lebegue, C. M. Araujo, D. Y. Kim, M. Ramzan, H. K. Mao and R. Ahuja, *Proc. Natl. Acad. Sci. U. S. A.*, 2012, **109**, 9766–9769.

43 C.-S. Zha, Z. Liu and R. J. Hemley, *Phys. Rev. Lett.*, 2012, **108**, 146402.

44 I. Amato, *Nature*, 2012, **486**, 174–176.

45 Y. Song and M. R. Manaa, *J. Phys. Chem. C*, 2012, **116**, 2059–2060.

46 W. L. Mao, H. K. Mao, A. F. Goncharov, V. V. Struzhkin, Q. Z. Guo, J. Z. Hu, J. F. Shu, R. J. Hemley, M. Somayazulu and Y. S. Zhao, *Science*, 2002, **297**, 2247–2249.

47 Alanates, borohydrides and amides belong to complex hydride described above.

48 In consideration of light-weight hydrides with reasonable hydrogen content, we only included alkali and alkaline earth metals up to 4th row elements as well as AlH_3. KH was not included due to the low weight content of hydrogen. BeH_2 was excluded due to the toxicity of Be that limits the practical application.

49 A. Lazicki, P. Loubeyre, F. Occelli, R. J. Hemley and M. Mezouar, *Phys. Rev. B: Condens. Matter Mater. Phys.*, 2012, **85**, 054103.

50 A. C. Ho, R. C. Hanson and A. Chizmeshya, *Phys. Rev. B: Condens. Matter Mater. Phys.*, 1997, **55**, 14818–14829.

51 P. Loubeyre, R. Le Toullec, M. Hanfland, L. Ulivi, F. Datchi and D. Hausermann, *Phys. Rev. B: Condens. Matter Mater. Phys.*, 1998, **57**, 10403–10406.

52 S. Lebegue, M. Alouani, B. Arnaud and W. E. Pickett, *Europhys. Lett.*, 2003, **63**, 562–568.

53 T. Ogitsu, E. Schwegler, F. Gygi and G. Galli, *Phys. Rev. Lett.*, 2003, **91**, 214506.

54 Y. Wang, R. Ahuja and B. Johansson, *Phys. Status Solidi B*, 2003, **235**, 470–473.

55 W. Yu, C. Jin and A. Kohlmeyer, *J. Phys.: Condens. Matter*, 2007, **19**, 086209.

56 J. Zhang, L. Zhang, T. Cui, Y. Li, Z. He, Y. Ma and G. Zou, *Phys. Rev. B: Condens. Matter Mater. Phys.*, 2007, **75**, 104115.

57 E. Zurek, R. Hoffmann, N. W. Ashcroft, A. R. Oganov and A. O. Lyakhov, *Proc. Natl. Acad. Sci. U. S. A.*, 2009, **106**, 17640–17643.

58 J. Hama and N. Kawakami, *Phys. Lett. A*, 1988, **126**, 348–352.

59 A. Lazicki, P. Loubeyre, F. Occelli, R. J. Hemley and M. Mezouar, *Phys. Rev. B: Condens. Matter Mater. Phys.*, 2012, **85**, 054103.

60 S. J. Duclos, Y. K. Vohra, A. L. Ruoff, S. Filipek and B. Baranowski, *Phys. Rev. B: Condens. Matter Mater. Phys.*, 1987, **36**, 7664–7667.

61 P. Baettig and E. Zurek, *Phys. Rev. Lett.*, 2011, **106**, 237002.

62 G. Wu, J. Zhang, Q. Li, Y. Wu, K. Chou and X. Bao, *Comput. Mater. Sci.*, 2010, **49**, S144–S149.

63 K.-F. Aguey-Zinsou and J.-R. Ares-Fernandez, *Energy Environ. Sci.*, 2010, **3**, 526–543.

64 H. Kohlmann, Y. Zhao, M. F. Nicol and J. McClure, *Z. Kristallogr.*, 2008, **223**, 706–710.

65 M. Bortz, B. Bertheville, G. Bottger and K. Yvon, *J. Alloys Compd.*, 1999, **287**, L4–L6.

66 P. Vajeeston, P. Ravindran, A. Kjekshus and H. Fjellvag, *Phys. Rev. Lett.*, 2002, **89**, 175506.

67 P. Vajeeston, P. Ravindran, B. C. Hauback, H. Fjellvag, A. Kjekshus, S. Furuseth and M. Hanfland, *Phys. Rev. B: Condens. Matter Mater. Phys.*, 2006, **73**, 224102.

68 S. Cui, W. Feng, H. Hu, Z. Feng and Y. Wang, *Solid State Commun.*, 2008, **148**, 403–405.

69 D. Moser, G. Baldissin, D. J. Bull, D. J. Riley, I. Morrison, D. K. Ross, W. A. Oates and D. Noreus, *J. Phys.: Condens. Matter*, 2011, **23**, 305403.

70 V. C. Y. Kong, D. W. Kirk, F. R. Foulkes and J. T. Hinatsu, *Int. J. Hydrogen Energy*, 2003, **28**, 205–214.

71 J. F. Mao, Z. P. Guo, X. B. Yu and H. K. Liu, *J. Phys. Chem. C*, 2011, **115**, 9283–9290.

72 B. Li, Y. Li, K. Yang, Q. Cui, Y. Ma and G. Zou, *J. Phys.: Condens. Matter*, 2007, **19**, 226205.

73 J. S. Tse, D. D. Klug, S. Desgreniers, J. S. Smith, R. Flacau, Z. Liu, J. Hu, N. Chen and D. T. Jiang, *Phys. Rev. B: Condens. Matter Mater. Phys.*, 2007, **75**, 134108.

74 Y. W. Li, B. Li, T. Cui, Y. Li, L. J. Zhang, Y. M. Ma and G. T. Zou, *J. Phys.: Condens. Matter*, 2008, **20**, 045211.

75 J. Graetz and J. J. Reilly, *J. Phys. Chem. B*, 2005, **109**, 22181–22185.

76 J. Graetz, J. J. Reilly, V. A. Yartys, J. P. Maehlen, B. M. Bulychev, V. E. Antonov, B. P. Tarasov and I. E. Gabis, *J. Alloys Compd.*, 2011, **509**, S517–S528.

77 S. K. Konovalov and B. M. Bulychev, *Inorg. Chem.*, 1995, **34**, 172–175.

78 R. Zidan, B. L. Garcia-Diaz, C. S. Fewox, A. C. Stowe, J. R. Gray and A. G. Harter, *Chem. Commun.*, 2009, 3717–3719.

79 I. N. Goncharenko, V. P. Glazkov, A. V. Irodova and V. A. Somenkov, *Physica B*, 1991, **174**, 117–120.

80 H. W. Brinks, A. Istad-Lem and B. C. Hauback, *J. Phys. Chem. B*, 2006, **110**, 25833–25837.

81 J. Graetz and J. J. Reilly, *J. Alloys Compd.*, 2006, **424**, 262–265.

82 H. W. Brinks, C. Brown, C. M. Jensen, J. Graetz, J. J. Reilly and B. C. Hauback, *J. Alloys Compd.*, 2007, **441**, 364–367.

83 H. W. Brinks, W. Langley, C. M. Jensen, J. Graetz, J. J. Reilly and B. C. Hauback, *J. Alloys Compd.*, 2007, **433**, 180–183.

84 J. Graetz, J. J. Reilly, J. G. Kulleck and R. C. Bowman, *J. Alloys Compd.*, 2007, **446**, 271–275.

85 V. A. Yartys, R. V. Denys, J. P. Maehlen, C. Frommen, M. Fichtner, B. M. Bulychev and H. Emerich, *Inorg. Chem.*, 2007, **46**, 1051–1055.

86 Y. Wang, J.-A. Yan and M. Y. Chou, *Phys. Rev. B: Condens. Matter Mater. Phys.*, 2008, **77**, 014101.

87 F. S. Manciu, L. Reza, W. G. Durrer, A. Bronson, D. Lacina and J. Graetz, *J. Raman Spectrosc.*, 2011, **42**, 512–516.

88 J. Graetz, S. Chaudhuri, Y. Lee, T. Vogt, J. T. Muckerman and J. J. Reilly, *Phys. Rev. B: Condens. Matter Mater. Phys.*, 2006, **74**, 214114.

89 I. Goncharenko, M. I. Eremets, M. Hanfland, J. S. Tse, M. Amboage, Y. Yao and I. A. Trojan, *Phys. Rev. Lett.*, 2008, **100**, 045504.

90 M. Tkacz, T. Palasyuk, J. Graetz and S. Saxena, *J. Raman Spectrosc.*, 2008, **39**, 922–927.

91 P. Vajeeston, P. Ravindran and H. Fjellvag, *Chem. Mater.*, 2008, **20**, 5997–6002.

92 V. Drozd, S. Garimella, S. Saxena, J. Chen and T. Palasyuk, *J. Phys. Chem. C*, 2012, **116**, 3808–3816.

93 A. Andreasen, T. Vegge and A. S. Pedersen, *J. Solid State Chem.*, 2005, **178**, 3672–3678.

94 V. P. Balema, V. K. Pecharsky and K. W. Dennis, *J. Alloys Compd.*, 2000, **313**, 69–74.

95 X. Ke and C. Chen, *Phys. Rev. B: Condens. Matter Mater. Phys.*, 2007, **76**, 024112.

96 M. Yoshino, K. Komiya, Y. Takahashi, Y. Shinzato, H. Yukawa and M. Morinaga, *J. Alloys Compd.*, 2005, **404**, 185–190.

97 Some derivative lithium aluminum hydrides, such as Li_3AlH_6, were also studied under high pressures. Considering only one such high-P study available (R. S. Kumar, *et al.*, *Chem. Phys. Lett.*, 2008, **460**, 442) and the intermediate nature in the hydrogen cycling of $LiAlH_4$ (see reaction 2), the review of such alanates is not included here.

98 B. C. Hauback, H. W. Brinks and H. Fjellvag, *J. Alloys Compd.*, 2002, **346**, 184–189.

99 A. V. Talyzin and B. Sundqvist, *Phys. Rev. B: Condens. Matter Mater. Phys.*, 2004, **70**, 180101.

100 R. S. Chellappa, D. Chandra, S. A. Gramsch, R. J. Hemley, J.-F. Lin and Y. Song, *J. Phys. Chem. B*, 2006, **110**, 11088–11097.

101 M. P. Pitt, D. Blanchard, B. C. Hauback, H. Fjellvag and W. G. Marshall, *Phys. Rev. B: Condens. Matter Mater. Phys.*, 2005, **72**, 214113.

102 P. Vajeeston, P. Ravindran, R. Vidya, H. Fjellvag and A. Kjekshus, *Phys. Rev. B: Condens. Matter Mater. Phys.*, 2003, **68**, 212101.

103 See P. Ravindran *et al.*, *J. Power Sources*, 2006, **159**, 88–99.

104 J. C. Fallas, W. M. Chien, D. Chandra, V. K. Kamisetty, E. D. Emmons, A. M. Covington, R. Chellappa, S. A. Gramsch, R. J. Hemley and H. Hagemann, *J. Phys. Chem. C*, 2010, **114**, 11991–11997.

105 T. J. Frankcombe, *Chem. Rev.*, 2012, **112**, 2164–2178.

106 A. V. Talyzin and B. Sundqvist, *High Pressure Res.*, 2006, **26**, 165–173.

107 R. S. Kumar, E. Kim, O. Tschauner, A. L. Cornelius, M. P. Sulic and C. M. Jensen, *Phys. Rev. B: Condens. Matter Mater. Phys.*, 2007, **75**, 174110.

108 R. S. Vennila, V. Drozd, L. George, S. K. Saxena, H. P. Liermann, H. Z. Liu, A. C. Stowe, P. Berseth, D. Anton and R. Zidan, *J. Alloys Compd.*, 2009, **473**, 576–578.

109 P. Vajeeston, P. Ravindran, R. Vidya, H. Fjellvag and A. Kjekshus, *Appl. Phys. Lett.*, 2003, **82**, 2257–2259.

110 E. H. Majzoub, K. F. McCarty and V. Ozolins, *Phys. Rev. B: Condens. Matter Mater. Phys.*, 2005, **71**, 024118.

111 B. C. Wood and N. Marzari, *Phys. Rev. Lett.*, 2009, **103**, 185901.

112 X. F. Zhou, X. Dong, Z. S. Zhao, A. R. Oganov, Y. J. Tian and H. T. Wang, *Appl. Phys. Lett.*, 2012, **100**, 061905.

113 H. W. Li, Y. G. Yan, S. Orimo, A. Zuttel and C. M. Jensen, *Energies*, 2011, **4**, 185–214.

114 $Mg(BH_4)_2$ was not included in the review considering that it has to prepared in the lab instead of from a commercial source, and there is only one high pressure study on it (see L. George, *et al.*, *J. Phys. Chem. C*, 2009, **113**, 486–492).

115 C. Li, P. Peng, D. W. Zhou and L. Wan, *Int. J. Hydrogen Energy*, 2011, **36**, 14512–14526.

116 J. P. Soulie, G. Renaudin, R. Cerny and K. Yvon, *J. Alloys Compd.*, 2002, **346**, 200–205.

117 Y. Filinchuk, D. Chernyshov and R. Cerny, *J. Phys. Chem. C*, 2008, **112**, 10579–10584.

118 A. V. Talyzin, O. Andersson, B. Sundqvist, A. Kurnosov and L. Dubrovinsky, *J. Solid State Chem.*, 2007, **180**, 510–517.

119 Y. Filinchuk, D. Chernyshov, A. Nevidomskyy and V. Dmitriev, *Angew. Chem., Int. Ed.*, 2008, **47**, 529–532.

120 V. Dmitriev, Y. Filinchuk, D. Chernyshov, A. V. Talyzin, A. Dzwilevski, O. Andersson and B. Sundqvist, *Phys. Rev. B: Condens. Matter Mater. Phys.*, 2008, **77**, 174112.

121 K. Miwa, N. Ohba, S. Towata, Y. Nakamori and S. Orimo, *Phys. Rev. B: Condens. Matter Mater. Phys.*, 2004, **69**, 245120.

122 Z. Lodziana and T. Vegge, *Phys. Rev. Lett.*, 2004, **93**, 145501.

123 A. Tekin, R. Caputo and A. Zuttel, *Phys. Rev. Lett.*, 2010, **104**, 215501.

124 Y. S. Yao and D. D. Klug, *Phys. Rev. B: Condens. Matter Mater. Phys.*, 2012, **86**, 064107.

125 U. B. Demirci, O. Akdim, J. Andrieux, J. Hannauer, R. Chamoun and P. Miele, *Fuel Cells*, 2010, **10**, 335–350.

126 S. S. Muir and X. D. Yao, *Int. J. Hydrogen Energy*, 2011, **36**, 5983–5997.

127 R. Retnamma, A. Q. Novais and C. M. Rangel, *Int. J. Hydrogen Energy*, 2011, **36**, 9772–9790.

128 D. M. F. Santos and C. A. C. Sequeira, *Renew. Sustainable Energy Rev.*, 2011, **15**, 3980–4001.

129 D. Chernyshov, A. Bosak, V. Dmitriev, Y. Filinchuk and H. Hagemann, *Phys. Rev. B: Condens. Matter Mater. Phys.*, 2008, **78**, 172104.

130 B. Sundqvist and O. Andersson, *Phys. Rev. B: Condens. Matter Mater. Phys.*, 2006, **73**, 092102.

131 D. G. Allis and B. S. Hudson, *Chem. Phys. Lett.*, 2004, **385**, 166–172.

132 O. A. Babanova, A. V. Soloninin, A. P. Stepanov, A. V. Skripov and Y. Filinchuk, *J. Phys. Chem. C*, 2010, **114**, 3712–3718.

133 C. M. Araujo, R. Ahuja, A. V. Talyzin and B. Sundqvist, *Phys. Rev. B: Condens. Matter Mater. Phys.*, 2005, **72**, 054125.

134 R. S. Kumar and A. L. Cornelius, *Appl. Phys. Lett.*, 2005, **87**, 261916.

135 E. Kim, R. Kumar, P. F. Weck, A. L. Cornelius, M. Nicol, S. C. Vogel, J. Zhang, M. Hartl, A. C. Stowe, L. Daemen and Y. Zhao, *J. Phys. Chem. B*, 2007, **111**, 13873–13876.

136 Y. Filinchuk, A. V. Talyzin, D. Chernyshov and V. Dmitriev, *Phys. Rev. B: Condens. Matter Mater. Phys.*, 2007, **76**, 092104.

137 G. Lee, J.-Y. Lee and J. S. Kim, *Solid State Commun.*, 2006, **139**, 516–521.

138 F. Yu, J. X. Sun, R. G. Tian, G. F. Ji and W. J. Zhu, *Chem. Phys.*, 2009, **362**, 135–139.

139 R. Caputo and A. Tekin, *J. Solid State Chem.*, 2011, **184**, 1622–1630.

140 C. Y. Zhu, Y. H. Liu, F. B. Tian and T. Cui, *Phys. Status Solidi B*, 2011, **248**, 1139–1142.

141 L. George, V. Drozd, H. Couvy, J. H. Chen and S. K. Saxena, *J. Chem. Phys.*, 2009, **131**, 074505.

142 E. A. Nickels, M. O. Jones, W. I. F. David, S. R. Johnson, R. L. Lowton, M. Sommariva and P. P. Edwards, *Angew. Chem., Int. Ed.*, 2008, **47**, 2817–2819.

143 K. C. Kim and D. S. Sholl, *J. Phys. Chem. C*, 2010, **114**, 678–686.

144 R. S. Kumar, E. Kim and A. L. Cornelius, *J. Phys. Chem. C*, 2008, **112**, 8452–8457.

145 E. Ronnebro and E. H. Majzoub, *J. Phys. Chem. B*, 2007, **111**, 12045–12047.

146 G. Barkhordarian, T. R. Jensen, S. Doppiu, U. Bosenberg, A. Borgschulte, R. Gremaud, Y. Cerenius, M. Dornheim, T. Klassen and R. Bormann, *J. Phys. Chem. C*, 2008, **112**, 2743–2749.

147 J. H. Kim, S. A. Jin, J. H. Shim and Y. W. Cho, *J. Alloys Compd.*, 2008, **461**, L20–L22.

148 J. H. Kim, S. A. Jin, J. H. Shim and Y. W. Cho, *Scr. Mater.*, 2008, **58**, 481–483.

149 Y. Kim, D. Reed, Y. S. Lee, J. Y. Lee, J. H. Shim, D. Book and Y. W. Cho, *J. Phys. Chem. C*, 2009, **113**, 5865–5871.

150 L. L. Wang, D. D. Graham, I. M. Robertson and D. D. Johnson, *J. Phys. Chem. C*, 2009, **113**, 20088–20096.

151 T. J. Frankcombe, *J. Phys. Chem. C*, 2010, **114**, 9503–9509.

152 J. F. Mao, Z. P. Guo, C. K. Poh, A. Ranjbar, Y. H. Guo, X. B. Yu and H. K. Liu, *J. Alloys Compd.*, 2010, **500**, 200–205.

153 K. Miwa, M. Aoki, T. Noritake, N. Ohba, Y. Nakamori, S. Towata, A. Zuttel and S. Orimo, *Phys. Rev. B: Condens. Matter Mater. Phys.*, 2006, **74**, 155122.

154 Y. Filinchuk, E. Ronnebro and D. Chandra, *Acta Mater.*, 2009, **57**, 732–738.

155 E. H. Majzoub and E. Ronnebro, *J. Phys. Chem. C*, 2009, **113**, 3352–3358.

156 M. Fichtner, K. Chlopek, M. Longhini and H. Hagemann, *J. Phys. Chem. C*, 2008, **112**, 11575–11579.

157 F. Buchter, Z. Lodziana, A. Rernhof, O. Friedrichs, A. Borgschulte, P. Mauron, A. Zuttel, D. Sheptyakov, G. Barkhordarian, R. Bormann, K. Chlopek, M. Fichtner, M. Sorby, M. Riktor, B. Hauback and S. Orimo, *J. Phys. Chem. B*, 2008, **112**, 8042–8048.

158 F. Buchter, Z. Lodziana, A. Remhof, O. Friedrichs, A. Borgschulte, P. Mauron, A. Zuttel, D. Sheptyakov, L. Palatinus, K. Chlopek, M. Fichtner, G. Barkhordarian, R. Bormann and B. C. Hauback, *J. Phys. Chem. C*, 2009, **113**, 17223–17230.

159 Y. S. Lee, Y. Kim, Y. W. Cho, D. Shapiro, C. Wolverton and V. Ozolins, *Phys. Rev. B: Condens. Matter Mater. Phys.*, 2009, **79**, 104107.

160 M. D. Riktor, M. H. Sorby, K. Chlopek, M. Fichtner, F. Buchter, A. Zuettel and B. C. Hauback, *J. Mater. Chem.*, 2007, **17**, 4939–4942.

161 L. George, V. Drozd, S. K. Saxena, E. G. Bardaji and M. Fichtner, *J. Phys. Chem. C*, 2009, **113**, 15087–15090.

162 A. Liu, S. T. Xie, S. Dabiran-Zohoory and Y. Song, *J. Phys. Chem. C*, 2010, **114**, 11635–11642.

163 A. Borgschulte, R. Gremaud, A. Zuttel, P. Martelli, A. Remhof, A. J. Ramirez-Cuesta, K. Refson, E. G. Bardaji, W. Lohstroh, M. Fichtner, H. Hagemann and M. Ernst, *Phys. Rev. B: Condens. Matter Mater. Phys.*, 2011, **83**, 024102.

164 P. C. Aeberhard, K. Refson, P. P. Edwards and W. I. F. David, *Phys. Rev. B: Condens. Matter Mater. Phys.*, 2011, **83**, 174102.

165 I. Llamas-Jansa, O. Friedrichs, M. Fichtner, E. G. Bardaji, A. Zuttel and B. C. Hauback, *J. Phys. Chem. C*, 2012, **116**, 13472–13479.

166 S. Y. Zaginaichenko, Z. A. Matysina, D. V. Schur and A. D. Zolotarenko, *Int. J. Hydrogen Energy*, 2012, **37**, 7565–7578.

167 A. Michigoe, T. Hasegawa, N. Ogita, T. Ichikawa, Y. Kojima, S. Isobe and M. Udagawa, *J. Phys. Soc. Jpn.*, 2012, **81**, 094603.

168 J. C. Wang, Y. Du, H. H. Xu, C. Jiang, Y. Kong, L. X. Sun and Z. K. Liu, *Phys. Rev. B: Condens. Matter Mater. Phys.*, 2011, **84**, 024107.

169 P. Chen, Z. T. Xiong, J. Z. Luo, J. Y. Lin and K. L. Tan, *Nature*, 2002, **420**, 302–304.

170 D. H. Gregory, *J. Mater. Chem.*, 2008, **18**, 2321–2330.

171 R. S. Chellappa, D. Chandra, M. Somayazulu, S. A. Gramsch and R. J. Hemley, *J. Phys. Chem. B*, 2007, **111**, 10785–10789.

172 X. L. Huang, D. Li, F. F. Li, X. L. Jin, S. Q. Jiang, W. B. Li, X. Y. Yang, Q. Zhou, B. Zou, Q. L. Cui, B. B. Liu and T. Cui, *J. Phys. Chem. C*, 2012, **116**, 9744–9749.

173 D. Prasad, N. W. Ashcroft and R. Hoffmann, *J. Phys. Chem. A*, 2012, **116**, 10027–10036.

174 Z. T. Xiong, J. J. Hu, G. T. Wu, Y. F. Liu and P. Chen, *Catal. Today*, 2007, **120**, 287–291.

175 D. A. Sheppard, M. Paskevicius and C. E. Buckley, *J. Phys. Chem. C*, 2011, **115**, 8407–8413.

176 A. Liu and Y. Song, *J. Phys. Chem. B*, 2011, **115**, 7–13.

177 Y. Zhong, H. Y. Zhou, C. H. Hu, D. H. Wang and A. R. Oganov, *J. Phys. Chem. C*, 2012, **116**, 8387–8393.

178 R. B. Liao, *Struct. Chem.*, 2012, **23**, 525–527.

179 T. W. Barbee III, A. K. McMahan, J. E. Klepeis and M. Van Schilfgaarde, *Phys. Rev. B: Condens. Matter Mater. Phys.*, 1997, **56**, 5148–5155.

180 Y. Song, C. Murli and Z. X. Liu, *J. Chem. Phys.*, 2009, **131**, 174506.
181 C. Murli and Y. Song, *J. Phys. Chem. B*, 2009, **113**, 13509–13515.
182 A. Torabi, Y. Song and V. N. Staroverov, *J. Phys. Chem. C*, 2013, **117**, 2210–2215.
183 K. Abe and N. W. Ashcroft, *Phys. Rev. B: Condens. Matter Mater. Phys.*, 2011, **84**, 094108.
184 Y. S. Yao and R. Hoffmann, *J. Am. Chem. Soc.*, 2011, **133**, 21002–21009.
185 K. Yamauchi, I. Hamada, H. B. Huang and T. Oguchi, *Appl. Phys. Lett.*, 2011, **99**, 181904.
186 Y. F. Liang and J. S. Tse, *J. Phys. Chem. C*, 2012, **116**, 2146–2152.
187 T. B. Marder, *Angew. Chem., Int. Ed.*, 2007, **46**, 8116–8118.
188 B. Peng and J. Chen, *Energy Environ. Sci.*, 2008, **1**, 479–483.
189 C. W. Hamilton, R. T. Baker, A. Staubitz and I. Manners, *Chem. Soc. Rev.*, 2009, **38**, 279–293.
190 N. C. Smythe and J. C. Gordon, *Eur. J. Inorg. Chem.*, 2010, 509–521.
191 A. Staubitz, A. P. M. Robertson and I. Manners, *Chem. Rev.*, 2010, **110**, 4079–4124.
192 Z. Li, G. Zhu, G. Lu, S. Qiu and X. Yao, *J. Am. Chem. Soc.*, 2010, **132**, 1490–1491.
193 Y. Zhang, K. Shimoda, T. Ichikawa and Y. Kojima, *J. Phys. Chem. C*, 2010, **114**, 14662–14664.
194 W. Osborn, T. Sadowski and L. L. Shaw, *Scr. Mater.*, 2011, **64**, 737–740.
195 Z. T. Xiong, C. K. Yong, G. T. Wu, P. Chen, W. Shaw, A. Karkamkar, T. Autrey, M. O. Jones, S. R. Johnson, P. P. Edwards and W. I. F. David, *Nat. Mater.*, 2008, **7**, 138–141.
196 M. E. Bowden, G. J. Gainsford and W. T. Robinson, *Aust. J. Chem.*, 2007, **60**, 149–153.
197 D. G. Allis, M. E. Kosmowski and B. S. Hudson, *J. Am. Chem. Soc.*, 2004, **126**, 7756–7757.
198 N. J. Hess, M. E. Bowden, V. M. Parvanov, C. Mundy, S. M. Kathmann, G. K. Schenter and T. Autrey, *J. Chem. Phys.*, 2008, **128**, 034508.
199 H. Cho, W. J. Shaw, V. Parvanov, G. K. Schenter, A. Karkamkar, N. J. Hess, C. Mundy, S. Kathmann, J. Sears, A. S. Lipton, P. D. Ellis and S. T. Autrey, *J. Phys. Chem. A*, 2008, **112**, 4277–4283.
200 S. M. Kathmann, V. Parvanov, G. K. Schenter, A. C. Stowe, L. L. Daemen, M. Hartl, J. Linehan, N. J. Hess, A. Karkamkar and T. Autrey, *J. Chem. Phys.*, 2009, **130**, 024507.
201 C. Ziparo, D. Colognesi, A. Giannasi and M. Zoppi, *J. Phys. Chem. A*, 2012, **116**, 8827–8832.
202 Q. Song, Y. Q. Hou, L. S. Li, Z. Y. Jiang, B. Zhou and X. D. Zhang, *Phys. B: Condens. Matter*, 2012, **407**, 565–570.
203 W. T. Klooster, T. F. Koetzle, P. E. M. Siegbahn, T. B. Richardson and R. H. Crabtree, *J. Am. Chem. Soc.*, 1999, **121**, 6337–6343.
204 R. Custelcean and Z. A. Dreger, *J. Phys. Chem. B*, 2003, **107**, 9231–9235.
205 S. Trudel and D. F. R. Gilson, *Inorg. Chem.*, 2003, **42**, 2814–2816.
206 Y. Lin, W. L. Mao, V. Drozd, J. Chen and L. L. Daemen, *J. Chem. Phys.*, 2008, **129**, 234509.
207 S. Xie, Y. Song and Z. Liu, *Can. J. Chem.*, 2009, **87**, 1235–1247.
208 Y. Filinchuk, A. H. Nevidomskyy, D. Chernyshov and V. Dmitriev, *Phys. Rev. B: Condens. Matter Mater. Phys.*, 2009, **79**, 214111.
209 J. Chen, H. Couvy, H. Liu, V. Drozd, L. L. Daemen, Y. Zhao and C.-C. Kao, *Int. J. Hydrogen Energy*, 2010, **35**, 11064–11070.
210 R. S. Kumar, X. Z. Ke, J. Z. Zhang, Z. J. Lin, S. C. Vogel, M. Hartl, S. Sinogeikin, L. Daemen, A. L. Cornelius, C. F. Chen and Y. S. Zhao, *Chem. Phys. Lett.*, 2010, **495**, 203–207.
211 L. Wang, K. Bao, X. Meng, X. Wang, T. Jiang, T. Cui, B. Liu and G. Zou, *J. Chem. Phys.*, 2011, **134**, 024517.
212 O. Andersson, Y. Filinchuk, V. Dmitriev, I. Quwar, A. V. Talyzin and B. Sundqvist, *Phys. Rev. B: Condens. Matter Mater. Phys.*, 2011, **84**, 024115.
213 S. Najiba, J. H. Chen, V. Drozd, A. Durygin and Y. Z. Sun, *J. Appl. Phys.*, 2012, **111**, 112618.
214 A. Liu and Y. Song, *J. Phys. Chem. C*, 2012, **116**, 2123–2131.
215 Y. Lin, H. W. Ma, C. W. Matthews, B. Kolb, S. Sinogeikin, T. Thonhauser and W. L. Mao, *J. Phys. Chem. C*, 2012, **116**, 2172–2178.
216 I. Kupenko, L. Dubrovinsky, V. Dmitriev and N. Dubrovinskaia, *J. Chem. Phys.*, 2012, **137**, 074506.
217 W. L. Mao, C. A. Koh and E. D. Sloan, *Phys. Today*, 2007, **60**, 42–47.
218 V. V. Struzhkin, B. Militzer, W. L. Mao, H. K. Mao and R. J. Hemley, *Chem. Rev.*, 2007, **107**, 4133–4151.
219 T. A. Strobel, K. C. Hester, C. A. Koh, A. K. Sum and E. D. Sloan, *Chem. Phys. Lett.*, 2009, **478**, 97–109.
220 See B. A. Chidester and T. A. Strobel, *J. Phys. Chem. A*, 2011, **115**, 10433–10437.
221 M. S. Somayazulu, L. W. Finger, R. J. Hemley and H. K. Mao, *Science*, 1996, **271**, 1400–1402.
222 M. S. Somayazulu, R. J. Hemley, A. F. Goncharov, H. K. Mao and L. W. Finger, *Eur. J. Solid State Inorg. Chem.*, 1997, **34**, 705–713.
223 W. L. Mao, V. V. Struzhkin, H. K. Mao and R. J. Hemley, *Chem. Phys. Lett.*, 2005, **402**, 66–70.
224 Q. Li and T. Thonhauser, *J. Phys.: Condens. Matter*, 2012, **24**, 424204.
225 W. L. Mao and H. K. Mao, *Proc. Natl. Acad. Sci. U. S. A.*, 2004, **101**, 708–710.
226 F. B. Su, C. L. Bray, B. O. Carter, G. Overend, C. Cropper, J. A. Iggo, Y. Z. Khimyak, A. M. Fogg and A. I. Cooper, *Adv. Mater.*, 2009, **21**, 2382–2386.
227 S. Y. Willow and S. S. Xantheas, *Chem. Phys. Lett.*, 2012, **525–526**, 13–18.
228 Y. H. Hu and E. Ruckenstein, *Angew. Chem., Int. Ed.*, 2006, **45**, 2011–2013.
229 W. L. Vos, L. W. Finger, R. J. Hemley and H. K. Mao, *Phys. Rev. Lett.*, 1993, **71**, 3150–3153.

230 W. L. Vos, L. W. Finger, R. J. Hemley and H. K. Mao, *Chem. Phys. Lett.*, 1996, **257**, 524–530.

231 K. A. Lokshin, Y. S. Zhao, D. W. He, W. L. Mao, H. K. Mao, R. J. Hemley, M. V. Lobanov and M. Greenblatt, *Phys. Rev. Lett.*, 2004, **93**, 125503.

232 K. A. Lokshin and Y. S. Zhao, *Appl. Phys. Lett.*, 2006, **88**, 131909.

233 H. Hirai, S. Ohno, T. Kawamura, Y. Yamamoto and T. Yagi, *J. Phys. Chem. C*, 2007, **111**, 312–315.

234 S.-i. Machida, H. Hirai, T. Kawamura, Y. Yamamoto and T. Yagi, *J. Chem. Phys.*, 2008, **129**, 224505.

235 V. E. Antonov, V. S. Efimchenko and M. Tkacz, *J. Phys. Chem. B*, 2009, **113**, 779–785.

236 T. Nakayama, K. Koga and H. Tanaka, *J. Chem. Phys.*, 2009, **131**, 214506.

237 J. W. Wang, H. L. Lu and J. A. Ripmeester, *J. Am. Chem. Soc.*, 2009, **131**, 14132–14133.

238 L. Hakim, K. Koga and H. Tanaka, *Phys. Rev. B: Condens. Matter Mater. Phys.*, 2010, **82**, 144105.

239 S. Machida, H. Hirai, T. Kawamura, Y. Yamamoto and T. Yagi, *J. Phys. Chem. Solids*, 2010, **71**, 1324–1328.

240 T. Sugahara, J. C. Haag, A. A. Warntjes, P. S. R. Prasad, E. D. Sloan, C. A. Koh and A. K. Sum, *J. Phys. Chem. C*, 2010, **114**, 15218–15222.

241 V. S. Efimchenko, M. A. Kuzovnikov, V. K. Fedotov, M. K. Sakharov, S. V. Simonov and M. Tkacz, *J. Alloys Compd.*, 2011, **509**, S860–S863.

242 T. J. Frankcombe and G. J. Kroes, *Phys. Chem. Chem. Phys.*, 2011, **13**, 13410–13420.

243 Q. Li, B. Kolb, G. Roman-Perez, J. M. Soler, F. Yndurain, L. Z. Kong, D. C. Langreth and T. Thonhauser, *Phys. Rev. B: Condens. Matter Mater. Phys.*, 2011, **84**, 153103.

244 R. G. Grim, P. B. Kerkar, M. Shebowich, M. Arias, E. D. Sloan, C. A. Koh and A. K. Sum, *J. Phys. Chem. C*, 2012, **116**, 18557–18563.

245 H. Hirai, S. Kagawa, T. Tanaka, T. Matsuoka, T. Yagi, Y. Ohishi, S. Nakano, Y. Yamamoto and T. Irifune, *J. Chem. Phys.*, 2012, **137**, 074505.

246 H. L. Lu, J. W. Wang, C. L. Liu, C. I. Ratcliffe, U. Becker, R. Kumar and J. Ripmeester, *J. Am. Chem. Soc.*, 2012, **134**, 9160–9162.

247 J. Zhang, J. L. Kuo and T. Iitaka, *J. Chem. Phys.*, 2012, **137**, 084505.

248 R. V. Belosludov, O. S. Subbotin, H. Mizuseki, Y. Kawazoe and V. R. Belosludov, *J. Chem. Phys.*, 2009, **131**, 244510.

249 V. S. Efimchenko, V. E. Antonov, O. I. Barkalov, S. N. Klyamkin and M. Tkacz, *High Pressure Res.*, 2009, **29**, 250–253.

250 L. Hakim, K. Koga and H. Tanaka, *Phys. Rev. Lett.*, 2010, **104**, 115701.

251 T. A. Strobel, M. Somayazulu and R. J. Hemley, *J. Phys. Chem. C*, 2011, **115**, 4898–4903.

252 X.-J. Chen, V. V. Struzhkin, Y. Song, A. F. Goncharov, M. Ahart, Z. Liu, H.-k. Mao and R. J. Hemley, *Proc. Natl. Acad. Sci. U. S. A.*, 2008, **105**, 20–23.

253 O. Degtyareva, M. Martinez Canales, A. Bergara, X.-J. Chen, Y. Song, V. V. Struzhkin, H.-k. Mao and R. J. Hemley, *Phys. Rev. B: Condens. Matter Mater. Phys.*, 2007, **76**, 064123.

254 M. I. Eremets, I. A. Trojan, S. A. Medvedev, J. S. Tse and Y. Yao, *Science*, 2008, **319**, 1506–1509.

255 T. A. Strobel, A. F. Goncharov, C. T. Seagle, Z. X. Liu, M. Somayazulu, V. V. Struzhkin and R. J. Hemley, *Phys. Rev. B: Condens. Matter Mater. Phys.*, 2011, **83**, 144102.

256 T. A. Strobel, M. Somayazulu and R. J. Hemley, *Phys. Rev. Lett.*, 2009, **103**, 065701.

257 S. B. Wang, H. K. Mao, X. J. Chen and W. L. Mao, *Proc. Natl. Acad. Sci. U. S. A.*, 2009, **106**, 14763–14767.

258 X. Q. Chen, S. B. Wang, W. L. Mao and C. L. Fu, *Phys. Rev. B: Condens. Matter Mater. Phys.*, 2010, **82**, 104115.

259 G. Forte, G. G. N. Angilella, N. H. March and R. Pucci, *Phys. Lett. A*, 2010, **374**, 580–583.

260 Y. W. Li, G. Y. Gao, Q. A. Li, Y. M. Ma and G. T. Zou, *Phys. Rev. B: Condens. Matter Mater. Phys.*, 2010, **82**, 064104.

261 Y. W. Li, G. Y. Gao, Y. Xie, Y. M. Ma, T. A. Cui and G. T. Zou, *Proc. Natl. Acad. Sci. U. S. A.*, 2010, **107**, 15708–15711.

262 K. Michel, Y. D. Liu and V. Ozolins, *Phys. Rev. B: Condens. Matter Mater. Phys.*, 2010, **82**, 174103.

263 M. Ramzan, S. Lebegue and R. Ahuja, *Phys. Rev. B: Condens. Matter Mater. Phys.*, 2010, **81**, 233103.

264 Y. S. Yao and D. D. Klug, *Proc. Natl. Acad. Sci. U. S. A.*, 2010, **107**, 20893–20898.

265 K. V. Shanavas, H. K. Poswal and S. M. Sharma, *Solid State Commun.*, 2012, **152**, 873–877.

266 W. L. Yim, J. S. Tse and T. Iitaka, *Phys. Rev. Lett.*, 2010, **105**, 215501.

267 T. A. Strobel, X. J. Chen, M. Somayazulu and R. J. Hemley, *J. Chem. Phys.*, 2010, **133**, 164512.

268 A structural model was proposed, but no specific space group with atomic positions was reported.

269 G. H. Zhong, C. Zhang, X. J. Chen, Y. L. Li, R. Q. Zhang and H. Q. Lin, *J. Phys. Chem. C*, 2012, **116**, 5226–5235.

270 Y. Lin, W. L. Mao and H.-k. Mao, *Proc. Natl. Acad. Sci. U. S. A.*, 2009, **106**, 8113–8116.

271 S. Wang, W. L. Mao and T. Autrey, *J. Chem. Phys.*, 2009, **131**, 144508.

272 R. S. Chellappa, M. Somayazulu, V. V. Struzhkin, T. Autrey and R. J. Hemley, *J. Chem. Phys.*, 2009, **131**, 224515.

273 H. Chacham and B. Koiller, *Phys. Rev. B: Condens. Matter Mater. Phys.*, 1995, **52**, 6147–6149.

274 P. Loubeyre, R. Letoullec and J. P. Pinceaux, *Phys. Rev. Lett.*, 1994, **72**, 1360–1363.

275 L. Ulivi, R. Bini, H. J. Jodl, P. Loubeyre, R. LeToullec and F. Datchi, *J. Low Temp. Phys.*, 1998, **111**, 703–708.

276 L. Ulivi, R. Bini, P. Loubeyre, R. LeToullec and H. J. Jodl, *Phys. Rev. B: Condens. Matter Mater. Phys.*, 1999, **60**, 6502–6512.

277 L. Ulivi, R. Bini and M. Santoro, *Physica B*, 1999, **265**, 39–48.

278 F. Grazzi and L. Ulivi, *Europhys. Lett.*, 2000, **52**, 564–570.

279 F. Grazzi, M. Santoro, M. Moraldi and L. Ulivi, *Phys. Rev. B: Condens. Matter Mater. Phys.*, 2002, **66**, 144303.

280 F. Grazzi and L. Ulivi, *High Pressure Res.*, 2002, **22**, 17–21.

281 N. Matsumoto and H. Nagara, *J. Phys.: Condens. Matter*, 2007, **19**, 365237.

282 C. Cazorla and D. Errandonea, *Phys. Rev. B: Condens. Matter Mater. Phys.*, 2010, **81**, 104108.

283 Y. S. Yao and D. D. Klug, *Phys. Rev. B: Condens. Matter Mater. Phys.*, 2011, **83**, 020105.

284 F. Grazzi, M. Santoro, M. Moraldi and L. Ulivi, *Phys. Rev. Lett.*, 2001, **87**, 125506.

285 A. P. Jephcoat, M. Amboage and A. K. Kleppe, in *International Conference on High Pressure Science and Technology, Joint Airapt-22 and Hpcj-50*, ed. K. Takemura, IOP Publishing Ltd, Bristol, vol. 215, 2010.

286 M. Somayazulu, P. Dera, A. F. Goncharov, S. A. Gramsch, P. Liermann, W. Yang, Z. Liu, H. K. Mao and R. J. Hemley, *Nat. Chem.*, 2010, **2**, 50–53.

287 T. Kaewmaraya, D. Y. Kim, S. Lebegue, C. J. Pickard, R. J. Needs and R. Ahuja, *Phys. Rev. B: Condens. Matter Mater. Phys.*, 2011, **84**, 092101.

288 L. J. Florusse, C. J. Peters, J. Schoonman, K. C. Hester, C. A. Koh, S. F. Dec, K. N. Marsh and E. D. Sloan, *Science*, 2004, **306**, 469–471.

289 H. Lee, J. W. Lee, D. Y. Kim, J. Park, Y. T. Seo, H. Zeng, I. L. Moudrakovski, C. I. Ratcliffe and J. A. Ripmeester, *Nature*, 2005, **434**, 743–746.